Synthesis, Characterization, and Redox Behavior of New Selenium Coronands and of Copper(I) and Copper(II) Complexes of Selenium Coronands

Raymond J. Batchelor, Frederick W. B. Einstein, Ian D. Gay, Jian-Hua Gu, Seema Mehta, B. Mario Pinto,* and Xue-Min Zhou

Department of Chemistry, Simon Fraser University, Burnaby, British Columbia, V5A 1S6, Canada

Received November 19, 1999

The synthesis and characterization of new selenium coronands and of copper(I) and copper(II) complexes of selenium coronands are reported. Molecular structures in the solid state have been determined by X-ray crystallography. The molecular structures of 6,7,13,14-dibenzo-1,5,8,12-tetraselenacyclotetradecane (dibenzo-14Se4 (**1**)) and 1,5,9-triselenacyclododecane (12Se3 (**2**)) adopt conformations which maximize the number of possible gauche C−Se−C−C bond torsion angles. **1**: $T = 190$ K; orthorhombic, space group $Pca2_1$; fw = 552.19; $Z = 4$; $a = 9.645(3)$ Å; $b = 12.679(6)$ Å; $c = 15.332(4)$ Å; $V = 1874.9$ Å^3; $R_F = 0.027$ for 1732 data ($I_o \geq 2.5\sigma(I_o)$) and 200 variables. **2**: $T = 190$ K; orthorhombic, space group $Pn2_1a$; fw = 363.12; Z = 4; $a = 14.943(4)$ Å; $b = 5.638(2)$ Å; $c = 14.229(3)$ Å; $V = 1198.8$ Å^3; $R_F = 0.026$ for 862 data ($I_o \geq 2.5\sigma(I_o)$) and 111 variables. The molecular structures of 1,5-diselena-9,13-dithiacyclohexadecane (16Se2S2 (**3**)) and $[Cu(16Se2S2)][SO_3CF_3]_2$ (**4**) correspond to those displayed by both of the analogous tetrathia and tetraselena macrocycles. Compound **3** adopts a [3535] quadrangular conformation. Compound **4**, $[Cu(16Se4(OH)_2][SO_3CF_3]_2$ (**5**) (where $16Se4(OH)_2$ = *cis*-1,5,9,13-tetraselenacyclohexadecane-3,11-diol), and $[Cu(8Se2(OH))_2][SO_3CF_3]_2$ (**6**) (where 8Se2(OH) = 1,5-diselenacyclooctan-3-ol) have typical tetragonally distorted octahedral coordination environments of Cu(II). Compounds **4** and **5** both display a c,t,c configuration of the coronand. Compound **5** has only one hydroxyl group coordinated in an axial position, which requires that the corresponding Se−Cu−Se−C−C−C ring be locked into a boat rather than a chair conformation. The hydroxyl groups in **6** occupy the axial coordination positions. **3**: $T = 200$ K; monoclinic, space group $C2/c$; fw = 390.36; $Z = 12$; $a = 24.202(9)$ Å; $b = 18.005(7)$ Å; $c = 16.235(5)$ Å; $\beta = 138.23(3)°$; $V = 4713$ Å^3; $R_F = 0.052$ for 1881 data ($I_o \geq 2.5\sigma(I_o)$) and 172 variables. **4**: $T = 297$ K; monoclinic, space group $P2_1/n$; fw = 752.03; Z = 2; $a = 8.882(2)$ Å; $b = 10.874(2)$ Å; $c = 13.360(2)$ Å; $\beta = 97.95(2)°$; $V = 1277.9$ Å^3; $R_F = 0.028$ for 1610 data ($I_o \geq 2.5\sigma(I_o)$) and 176 variables. **5**: $T = 190$ K; monoclinic, space group $P2_1/n$; fw = 877.84; Z = 4; $a = 8.412(5)$ Å; $b = 20.924(5)$ Å; $c = 15.021(5)$ Å; $\beta = 100.82(4)°$; $V = 2597$ Å^3; $R_F = 0.059$ for 2152 data ($I_o \geq 2.5\sigma(I_o)$) and 185 variables. **6**: $T = 195$ K; monoclinic, space group $P2_1/c$; fw = 877.84; $Z = 2$; $a = 6.875(2)$ Å; $b = 10.945(2)$ Å; $c = 17.496(2)$ Å; $\beta = 96.76(2)°$; $V = 1307.3$ Å^3; $R_F = 0.023$ for 1816 data ($I_o \geq 2.5\sigma(I_o)$) and 159 variables. $[Cu(16Se2S2)][SO_3CF_3]$ (**7**) and $[Cu(16Se4(OH))][SO_3CF_3]$ (**8**) (where 16Se4(OH) = 1,5,9,13-tetraselenacyclohexadecan-3-ol) are both tetrahedral Cu(I) coronand complexes with typical t,t,t configurations. **7**: $T = 205$ K; triclinic, space group $P\bar{1}$; fw = 602.97; $Z = 2$; $a = 10.512(3)$ Å; $b = 10.674(2)$ Å; $c = 10.682(3)$ Å; $\alpha = 101.47(2)°$; $\beta = 116.82(2)°$; $\gamma = 93.59(2)°$; $V = 1032.3$ Å^3; $R_F = 0.029$ for 2237 data ($I_o \geq 2.5\sigma(I_o)$) and 264 variables. **8**: $T = 297$ K; monoclinic, space group $P2_1/n$; fw = 712.77; $Z = 4$; $a = 13.695(2)$ Å; $b = 11.202(2)$ Å; $c = 14.163(3)$ Å; $\beta = 92.35(2)°$; $V = 2170.9$ Å^3; $R_F = 0.035$ for 2086 data ($I_o \geq 2.5\sigma(I_o)$) and 189 variables. Compounds **5**, **6**, and **8** all display hydrogen bonding between hydroxyl groups and the $SO_3CF_3^-$ ions. Isotropic ^{13}C and ^{77}Se chemical shifts have been obtained in the solid state for **2**, **3**, 1,5,9,13-tetraselenacyclohexadecane-3,11-diol ($16Se4(OH)_2$ (**9**)), 1,5,9,13-tetraselenacyclohexadecan-3-ol (16Se4(OH) (**10**)), and the dicationic complex 1,5,-(diseleniacyclooctane trifluoromethanesulfonate ($8Se2(SO_3CF_3)_2$ (**11**)). In addition, the ^{77}Se chemical shift anisotropies have been determined for **10** and **11**. The dicationic compound **11** resonates at lower field, reflective of a contribution from the transannular Se−Se bond. The redox behavior of **1**−**8** has been examined by means of cyclic voltammetry. Redox behavior of the copper complexes **4**, **5**, and **6** indicates the presence of two different conformational isomers of the Cu(I) complexes that are oxidized at different potentials, analogous to Rorabacher's copper(II/I) complexes that follow a dual-pathway square-scheme mechanism. The quasi-reversible cyclic voltammograms observed for the Cu(II) complexes of selenium coronands reflect the configurational changes between Cu(II) complexes (octahedral or tetragonal configurations) and Cu(I) complexes (tetrahedral configurations) and indicate that the configurational changes are slower than the electron transfers to the electrode.

Introduction

There is a growing interest in chalcogen macrocycles as models for metalloenzymes and metalloproteins and in the structure and bonding of metal−chalcogen macrocyclic complexes.[1−3] The Cu(II/I) redox couple is of importance in biological systems, for example, metalloenzymes, where it is involved in biological oxidation−reduction processes. Of particular interest are the blue copper proteins, which include mononuclear copper proteins, and multicopper enzymes, which

* Corresponding author. E-mail: bpinto@sfu.ca. Tel.: 1-604-291-4327. Fax: 1-604-291-3765.

10.1021/ic991345p CCC: $19.00
Published on Web 05/19/2000

are found to exhibit unique spectral and redox properties. The importance of the Cu(II/I) redox couple in enzymes has stimulated investigations into the influence of macrocyclic ligands upon the nature, coordination geometry, reactivity, and electrochemical properties of the copper complexes.[1−3] The interesting coordination chemistry of thia macrocycles[4−8] has prompted our investigation of the chemistry of the selenium congeners. We have reported the synthesis and properties of various selenium coronands and described their metal ion complexes.[9−16] We have reported the structures of the Pd(II) complex of 1,5,9,13-tetraselenacyclohexadecane (16Se4)[13] and the Pd(II) complex of 1,5,9,13,17,21-hexaselenacyclotetracosane (24Se6).[13] We have also described a study of the adducts of 16Se4 with copper(I) triflate and mercury(II) cyanide,[14] as well as Cu(I), Cu(II), and Pd(II) complexes of other selenium coronands.[15] Other reports of complexes of 16Se4, with Rh(III), Co(III), and Ir(III),[17,18] with Pd(II) and Pt(II),[19] and with Ni(II), Ag(I), Cr(III), Ru(II), and Ru(III),[20−23] have also appeared. Transition metal ion complexation by mono- and diselena[24−26] and tetraselena[27−34] macrocyclic ligands containing additional heteroatoms has also been reported. Of particular relevance to the present work, we have described the unusual electron-transfer reaction of a Cu(II) complex of 16Se4.[12,16] We describe here the synthesis, characterization, redox properties, and X-ray crystal structures of the new selenium coronands 6,7,13,14-dibenzo-1,5,8,12-tetraselenacyclotetradecane (dibenzo-14Se4 (**1**)), 1,5,9-triselenacyclododecane (12Se3 (**2**)),[10] and 1,5-diselena-9,13-dithiacyclohexadecane (16Se2S2 (**3**)). (See Figure 1.) We also describe the synthesis, characterization, redox properties, and X-ray crystal structures of the Cu(II) complexes of 1,5-diselena-9,13-dithiacyclohexadecane ([Cu(16Se2S2)][SO_3CF_3]$_2$ (**4**)), *cis*-1,5,9,13-tetraselenacyclohexadecane-3,11-diol ([Cu(16Se4(OH)$_2$)][SO_3CF_3]$_2$ (**5**)), and 1,5-diselenacyclooctan-3-ol ([Cu(8Se2(OH))$_2$][SO_3CF_3]$_2$ (**6**)) and the Cu(I) complexes of 1,5-diselena-9,13-dithiacyclohexadecane ([Cu(16Se2S2)][SO_3CF_3] (**7**)) and 1,5,9,13-tetraselenacyclohexadecan-3-ol ([Cu(16Se4(OH))][SO_3CF_3] (**8**)). The isotropic ^{13}C and ^{77}Se chemical shifts obtained in the solid state for **2**, **3**, 1,5,9,13-tetraselenacyclohexadecan-3,11-diol (16Se4(OH)$_2$ (**9**)),[11] 1,5,9,13-tetraselenacyclohexadecan-3-ol (16Se4(OH) (**10**)),[11] and the dicationic compound 1,5-(diseleniacyclooctane trifluoromethanesulfonate (8Se2(SO_3CF_3)$_2$ (**11**)) are presented, as well as the ^{77}Se chemical shift anisotropies for **10** and **11**.

Since the redox behavior of Cu(I) and Cu(II) complexes of sulfur coronands is well characterized[35−40] and that of the corresponding selenium congeners is now being explored,[12,14,16] it is of some interest to investigate the properties of Cu complexes of coronands containing sulfur and selenium atoms (**4** and **7**). It is also of considerable interest to probe the effect of the pendant hydroxyl groups in the Cu complexes **5**, **6**, and **8** on the stability of these complexes and their redox properties.

Experimental Section

General Information. Analytical TLC was performed on precoated aluminum plates with Merck 60F-254 silica gel as the adsorbent. The developed plates were air-dried, exposed to UV light and/or sprayed with 10% H_2SO_4 in ethanol, and heated to 100 °C. Flash column chromatography was performed on Kieselgel 60 (230−400) according to a published procedure.[41] Solvents were distilled before use and were dried, as necessary, by literature procedures. Acetonitrile (CH_3CN;

(1) For example: Rorabacher, D. B.; Martin, M. J.; Koenigbauer, M. J.; Malik, M.; Schroeder, R. R.; Endicott, J. F.; Ochrymowycz, L. A. In *Copper Coordination Chemistry: Biochemical and Inorganic Perspectives*; Karlin, K. D., Zubieta, J., Eds.; Adenine Press: Guilderland, NY, 1983; p 167.
(2) For example: (a) LaCroix, L. B.; Randall, D. W.; Nersissian, A. M.; Hoitink, C. W. G.; Canters, G. W.; Valentine, J. S.; Solomon, E. I. *J. Am. Chem. Soc.* **1998**, *120*, 9621. (b) Solomon, E. I.; Penfield, K. W.; Gewirth, A. A.; Lowery, M. D.; Shadle, S. E.; Guckert, J. A.; LaCroix, L. B. *Inorg. Chim. Acta* **1996**, 67. (c) Guckert, J. A.; Lowery, M. D.; Solomon, E. I. *J. Am. Chem. Soc.* **1995**, *117*, 2817.
(3) For example: (a) Ambundo, E. A.; Deydier, M.-V.; Grall, A. J.; Aguera-Vega, N.; Dressel, L. T.; Cooper. T. H.; Heeg, M. J.; Ochrymowycz, L. A.; Rorabacher, D. B. *Inorg. Chem.* **1999**, *38*, 4233. (b) Krylova, K.; Kulatilleke, C. P.; Heeg, M. J.; Salhi, C. A.; Ochrymowycz, L. A.; Rorabacher, D. B. *Inorg. Chem.* **1999**, *38*, 4322.
(4) Rorabacher, D. B.; Bernado, M. M.; Vande Linde, A. M. Q.; Leggett, G. H.; Westerby, B. C.; Martin, M. J.; Ochrymowycz, L. A. *Pure Appl. Chem.* **1988**, *60*, 501.
(5) Schröder, M. *Pure Appl. Chem.* **1988**, *60*, 517.
(6) Cooper, S. R. *Acc. Chem. Res.* **1988**, *21*, 141.
(7) Blake, A. J.; Gould, R. O.; Greig, J. A.; Holder, A. J.; Hyde, T. I.; Schröder, M. *J. Chem. Soc., Chem. Commun*. **1989**, 876.
(8) Blake, A. J.; Schröder, M. *Adv. Inorg. Chem.* **1990**, *35*, 1.
(9) Batchelor, R. J.; Einstein, F. W. B.; Gay, I. D.; Gu, J. H.; Johnston, B. D.; Pinto, B. M. *J. Am Chem. Soc*. **1989**, *111*, 6582.
(10) Cordova-Reyes, I.; VandenHoven, E.; Mohammed, A.; Pinto, B. M. *Can. J. Chem.* **1995**, *73*, 113.
(11) Cordova-Reyes, I.; Hu, H.; Gu, J.-H.; VandenHoven, E.; Mohammed, A.; Holdcroft, S.; Pinto, B. M. *Can. J. Chem*. **1996**, *74*, 533.
(12) Batchelor, R. J.; Einstein, F. W. B.; Gay, I. D.; Gu, J.-H.; Pinto, B. M.; Zhou, X.-M. *J. Am. Chem. Soc.* **1990**, *112*, 3706.
(13) Batchelor, R. J.; Einstein, F. W. B.; Gay, I. D.; Gu, J.-H.; Pinto, B. M.; Zhou, X.-M. *Inorg. Chem*. **1996**, *35*, 3667.
(14) Batchelor, R. J.; Einstein, F. W. B.; Gay, I. D.; Gu, J.-H.; Pinto, B. M. *J. Organomet. Chem*. **1991**, *411*, 147.
(15) Pinto, B. M.; Batchelor, R. J.; Einstein, F. W. B.; Gay, I. D.; Gu, J.; Zhou, X.-M. *Abstracts of Papers*, 76th Conference of the Canadian Society for Chemistry, Sherbrooke, Quebec, Canada, June 1993. Abstr. 683.
(16) Batchelor, R. J.; Einstein, F. W. B.; Gay, I. D.; Gu, J.-H.; Pinto, B. M.; Zhou, X.-M., *Can. J. Chem.*, in press.
(17) Kelly, P. F.; Levason, W.; Reid, G.; Williams, D. J. J. *Chem. Soc., Chem. Commun*. **1993**, 1716.
(18) Levason, W.; Quirk, J. J.; Reid, G. *J. Chem. Soc., Dalton Trans*. **1996**, 3713.
(19) Champness, N. R.; Kelly, P. F.; Levason, W.; Reid, G.; Slawin, A. M. Z.; Williams, D. J. *Inorg. Chem*. **1995**, *34*, 651.
(20) Booth, D. G.; Levason, W.; Quirk, J. J.; Reid, G.; Smith, S. M. *J. Chem. Soc., Dalton Trans.* **1997**, 3493.
(21) Davies, M. K.; Levason, W.; Reid, G. *J. Chem. Soc., Dalton Trans*. **1998**, 2185.
(22) Levason, W.; Reid G.; Smith, S. M. *Polyhedron* **1997**, *16*, 4253.
(23) Levason, W.; Quirk, J. J.; Reid, G.; Smith, S. M. *J. Chem. Soc., Dalton Trans*. **1997**, 3719.
(24) Xu, H.; Li, W.; Liu, X. *Youji Huaxue* **1993**, *13*, 52.
(25) Kumagai, T.; Akabori, S. *Chem. Lett*. **1989**, 1667.
(26) Bornet, C.; Amardeil, R.; Meunier, P.; Daran, J. C. *J. Chem. Soc., Dalton Trans*. **1999**, 1039.
(27) Li, W.-P.; Wu, J.; Zhang, J.-G.; Liu, X.-F.; Xu, H.-S. *Youji Huaxue* **1996**, *16*, 436.
(28) Li, W.-P.; Liu, X.-F.; Xu, H.-S. *Huaxue Xuebao* **1994**, *52*, 1082.
(29) Li, W.-P.; Liu, X.-F.; Lu, X.-R.; Xu, H.-S. *Gaodeng Xuexiao Huaxue Xuebao* **1994**, *52*, 1082.
(30) Li, W.-P.; Wu, J.; Liu, X.-F.; Xu, H.-S. *Gaodeng Xuexiao Huaxue Xuebao* **1995**, *16*, 1558.
(31) Huang, Y.-Q.; Hu, S.-Z.; Li, W.-P.; Liu, X.-F.; Xu, H.-S. *Jiegou Huaxue* **1995**, *14*, 267.
(32) Li, W.-P.; Liu, X.-F.; Xu, H.-S.; Huang, Y.-Q.; Hu, S.-Z. *Chin. J. Chem*. **1995**, *13*, 47.
(33) Liu, Y.; Dong, S.-P.; Inoue, Y.; Wada, T. J. *Chem. Res., Synop*. **1999**, 284.
(34) Mazouz, A.; Meunier, P.; Kubicki, M. M.; Hanquet, B.; Amardeil, C. B.; Zahidi, A. *J. Chem. Soc., Dalton Trans.* **1997**, 1043.
(35) Cornfield, P. W. R.; Ceccarelli, C.; Glick, M. D.; Moy, I. W.-Y.; Ochrymowycz, L. A.; Rorabacher, D. B. *J. Am. Chem. Soc.* **1985**, *107*, 2399.
(36) Cooper, S. R.; Hartman, J. R. *J. Am. Chem. Soc.* **1986**, *108*, 1202.
(37) Rorabacher, D. B.; Ochrymowycz, L. A.; Glick, M. D. *Inorg. Chem.* **1983**, *22*, 3661.
(38) Diaddario, L. L., Jr.; Dockal, E. R.; Glick, M. D.; Ochrymowycz, L. A.; Rorabacher, D. B. *Inorg. Chem.* **1985**, *24*, 356.
(39) Martin, M. J.; Endicott, J. F.; Ochrymowycz, L. A.; Rorabacher, D. B. *Inorg. Chem*. **1987**, *26*, 3012.
(40) Bernardo, M. M.; Heeg, M. J.; Schroeder, R. R.; Ochrymowycz, L. A.; Rorabacher, D. B. *Inorg. Chem*. **1992**, *31*, 191.
(41) Still, W. C.; Kahn, M.; Mitra, M. *J. Org. Chem.* **1978**, *43*, 2923.

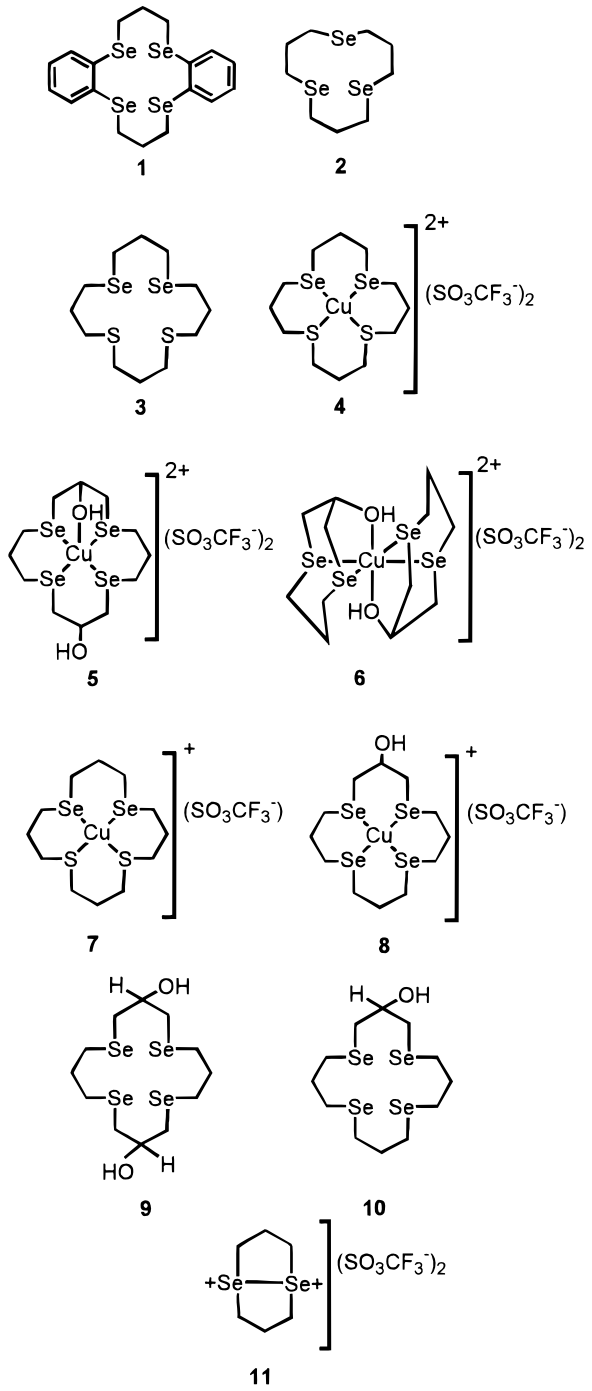

Figure 1. Selenium coronands and Cu(II) and Cu(I) complexes.

Fisher or Caledon, AR or HPLC grade) was refluxed with CaH_2 and distilled under N_2 before use. Tetraethylammonium perchlorate (Et_4NClO_4 (TEAP); Kodak) was dried under vacuum at 70 °C. (***Warning! Perchlorate salts are potentially explosive and should be handled with care!***)[42] Nitrosonium tetrafluoroborate ($NOBF_4$; Aldrich) was sublimed at 100 °C under vacuum, sealed in a vial, and kept in a freezer (−20 °C) until use. Chemical ionization mass spectra were recorded on a Hewlett-Packard HP-5899 mass spectrometer with isobutane as the reacting gas. Microanalyses were performed by M. K. Yang of the Microanalytical Laboratory of Simon Fraser University.

Spectroscopy. ^1H NMR spectra were recorded on a Bruker SY-100 spectrometer at 100 MHz, and coupling constants were obtained from a first-order analysis of the spectra. ^{13}C NMR solution-phase spectra were recorded on a Bruker AMX-400 NMR spectrometer at 100.6 MHz. Chemical shifts are given in ppm with respect to $SiMe_4$.

Solid-state NMR spectra were recorded on an instrument (built in house), operating at a field of 1.4 or 3.5 T. This produced resonance frequencies of 11.4 or 28.5 MHz and 15.1 or 37.5 MHz for ^{77}Se and ^{13}C, respectively. Spectra were excited by using single-contact Hartmann−Hahn cross polarization. The matched radio frequency field strengths were 40 and 50 kHz for ^{77}Se and ^{13}C, respectively. The same field strengths were used for proton decoupling during data acquisition. Samples were spun at the magic angle at frequencies of 2−3 kHz. The magic angle was correctly set within ±0.1° by optimizing the line width on well-crystallized samples of $(t\text{-}Bu_2Sn)_2Se_2$ and $H_2C_2O_4{\cdot}2H_2O$. Chemical shifts were measured relative to long cylindrical samples of aqueous H_2SeO_3 and C_6H_6. These were converted to shifts based on the standard Me_2Se and TMS scales by use of literature data.[43−46]

IR spectra were recorded on a Bomem FT-IR spectrometer. UV−visible spectra were measured on a Hewlett-Packard HP 89500 UV/vis chem station or a Hewlett-Packard HP 8452 diode array spectrophotometer. The temperature was controlled at 25 °C.

Electrochemistry. Cyclic voltammetry and electrolysis were performed on either a PAR model 170 electrochemistry system or a PAR model 173/175 electrochemistry system. Cyclic voltammetry was carried out with a three-electrode device. The reference electrode was an aqueous saturated calomel electrode (SCE) with a Luggin capillary. The working electrode was a platinum plate, and the counter electrode was a platinum wire. Before potential scanning, the solution which contained a selenium coronand (1 mM) and tetraethylammonium perchlorate (TEAP, 0.1 M) as the electrolyte was bubbled with N_2 for 15 min. An N_2 flow was kept above the surface of the solution after the bubbling to maintain a nitrogen atmosphere. The cyclic voltammograms of all selenium coronands were obtained from a single scan for every concentration and every scan rate, and the surface of the electrode was cleaned with a tissue between scans. The potential drop due to the liquid junction between the reference electrode and electrolyte was calibrated with ferrocene.

Controlled-potential electrolysis was carried out in a two-compartment electrochemical cell, which was partitioned by a sintered-glass disk. The working and counter electrodes were Pt gauze electrodes. The reference electrode was an aqueous saturated calomel electrode (SCE) with a Luggin capillary. TEAP (0.1 M) was used as the electrolyte. The solution was purged with the N_2 for 15 min before the electrolysis, and the N_2 flow was kept bubbling during electrolysis of the stirred solution.

Chemical Generation of Radical Cations. Stock solutions of $NOBF_4$ and the selenium coronands, in freshly distilled CH_3CN, were freshly prepared, the latter in a glovebag under N_2. Each selenium coronand solution (3 mL) was transferred with a pipet into a quartz UV cuvette which was then sealed with a septum. N_2 was bubbled through the solution for 15 min, after which the $NOBF_4$ solution was added to the stirred coronand solution with a 25 μL syringe. When half of the $NOBF_4$ solution had been added, the repeated scanning of the spectrum was commenced at 4, 60 and 300 s intervals, according to the stability of the particular radical cation.

Syntheses. 1,2-Bis((3-hydroxy-1-propyl)selenio)benzene (13). $NaBH_4$ (0.65 g, 20.0 mmol) in dry EtOH (20 mL) was added to poly(1,2-diseleniobenzene) (**12**)[47] (1.0 g, 4.0 mmol) in dry THF (50 mL). A clear light yellow solution was formed, to which 3-bromo-1-propanol (2.36 g, 20.0 mmol) in dry THF (30 mL) was added. The mixture was stirred at ambient temperature for 48 h, poured into water (150 mL), and extracted with CH_2Cl_2 (3 × 30 mL). The combined extracts were

(42) For example: (a) Wolsey, W. C. *J. Chem. Educ.* **1973**, *50*, A335. (b) Raymond, K. N. *Chem. Eng. News.* **1983**, *61* (Dec 5), 4.

(43) Hope, E. G.; Levason, W. *Coord. Chem. Rev.* **1993**, *122*, 109.
(44) Orrell, K. G. *Coord. Chem. Rev.* **1989**, *96*, 1−48.
(45) Günther, W. H. H. In *Organic Selenium Compounds: Their Chemistry and Biology*; Klayman, D. L., Günther, W. H. H., Eds.; John Wiley & Sons: New York, 1973; pp 1−12.
(46) Luthra, N. P.; Odom, J. D. In *The Chemistry of Organic Selenium and Tellurium Compounds*; Patai, S., Rappoport, Z., Eds.; John Wiley & Sons: New York, 1986; Vol. 1.
(47) Sandman, D. J.; Allen, G. W.; Acampora, L. A.; Stark, J. C.; Jansen, S.; Jones, M. T.; Ashwell, G. J.; Forman, B. M. *Inorg. Chem.* **1987**, *26*, 1664.

washed with water, dried (Na_2SO_4), and concentrated in vacuo to afford a light yellow oil. Purification by silica gel flash chromatography (hexane/ethyl acetate, 1:1) afforded **13** as a yellow oil (1.0 g, 66%). ^{1}H NMR ($CDCl_3$): δ 1.97 (4H, p, J = 6.6 Hz, $SeCH_2CH_2CH_2OH$), 2.72 (2H, m, OH's), 3.02 (4H, t, J = 6.6 Hz, $SeCH_2CH_2CH_2OH$), 3.78 (4H, t, J = 6.6 Hz, $SeCH_2CH_2CH_2OH$), 7.11−7.46 (4H, m, Ar). ^{13}C NMR ($CDCl_3$): δ 24.3 ($SeCH_2$'s), 32.3 (β-CH_2's), 62.3 ($-CH_2OH$), 127.3, 132.0, 134.9 (Ar). IR (neat): 3400 (br, ν(OH)), 3040 (ν(-ArH)), 2930, 2850 (s, ν(CH)), 1435 (s, δ(CH)), 1240, 1050 (s, ν(C−O)) cm^{-1}. MS: 352 ($M^{+\bullet}$). Anal. Calcd for $C_{12}H_{18}Se_2O_2$: C, 40.92; H, 5.15. Found: C, 41.08; H, 5.20.

1,2-Bis((3-chloro-1-propyl)selenio)benzene (14). A solution of 1,2-bis((3-hydroxy-1-propyl)selenio)benzene (**13**) (1.35 g, 4.0 mmol) in dry CH_2Cl_2 (5 mL) was added dropwise to thionyl chloride (10 mL). The mixture was refluxed for 1.5 h, and the thionyl chloride was removed in vacuo. The residue was diluted with water (50 mL) and extracted with CH_2Cl_2 (3 × 20 mL). The combined organic extracts were washed with water (3 × 20 mL), dried over Na_2SO_4, and concentrated in vacuo to yield a yellow oil. Purification by silica gel flash chromatography (hexane/ethyl acetate, 20:1) afforded **14** (420 mg, 31%). ^{1}H NMR ($CDCl_3$): δ 2.15 (4H, p, J = 6.6 Hz, $SeCH_2CH_2CH_2Cl$), 3.10 (4H, t, J = 6.9 Hz, $SeCH_2CH_2CH_2Cl$), 3.70 (4H, t, J = 6.3 Hz, $SeCH_2CH_2CH_2Cl$), 7.17−7.80 (4H, m, Ar). ^{13}C NMR ($CDCl_3$): δ 24.6 ($SeCH_2$'s), 32.4 (β-CH_2's), 44.3 ($-CH_2Cl$), 127.5, 132.1, 134.0 (Ar). IR (neat): 3040 (ν(ArH)), 2940 (s, δ(CH)), 1550 (s, ν(C═C), Ar) cm^{-1}. MS: 390 ($(M + H)^+$). Anal. Calcd for $C_{12}H_{17}Cl_2Se_2$: C, 37.11; H, 4.12. Found: C, 37.32; H, 4.10.

Dibenzo-14Se4 (1). $NaBH_4$ (160 mg, 4.21 mmol) in dry EtOH (5 mL) was added dropwise to poly(1,2-diseleniobenzene) (**12**)[47] (246 mg, 1.05 mmol) in dry THF (10 mL) at ambient temperature. 1,2-Bis((3-chloro-1-propyl)selenio)benzene (**14**) (340 mg, 0.87 mmol) in THF (20 mL) was added dropwise to the above solution. The reaction mixture was stirred at ambient temperature for 24 h, diluted with water (20 mL), and extracted with CH_2Cl_2 (3 × 20 mL). The combined extracts were washed with water (3 × 20 mL), dried over Na_2SO_4, and concentrated in vacuo to yield a thick orange oil. Purification by silica gel flash chromatography (hexane/ethyl acetate, 20:1) afforded **1** as yellowish crystals (290 mg, 60%) which were recrystallized from CH_2Cl_2/EtOAc. Mp: 171−172 °C. ^{1}H NMR ($CDCl_3$): δ 1.98 (4H, p, J = 7.1 Hz, $SeCH_2CH_2CH_2Se$), 3.02 (8H, t, J = 7.1 Hz, $SeCH_2CH_2CH_2Se$), 6.95−7.35 (8H, m, Ar). ^{13}C NMR ($CDCl_3$): δ 27.0 ($SeCH_2$'s), 29.3 (β-CH_2's), 127.3, 133.7, 134.1 (Ar). IR (KBr): 3030 (ν(ArH)), 2910 (s, ν(CH)), 1550 (ν(C═C)), 1210, 1020 cm^{-1}. UV (CH_2Cl_2), λ_{max} (ϵ): 256 nm (2.2×10^4), 274 nm (2.2×10^4). MS: 552 ($M^{+\bullet}$). Anal. Calcd for $C_{18}H_{20}Se_4$: C, 39.15; H, 3.65. Found: C, 39.10; H, 3.51.

1,3-Bis((3-mercaptopropyl)selenio)propane (16). $NaBH_4$ (1.2 g, 0.03 mol) in dry EtOH (15 mL) was added dropwise to 1,3-propanediyldiselenium cyanide (**15**)[48] (2.0 g, 0.08 mol) in dry THF (30 mL) at ambient temperature. 3-Chloropropanethiol (1.76 g, 0.02 mol) in THF (20 mL) was added dropwise to the above solution. The reaction mixture was stirred at ambient temperature for 96 h. The solution was concentrated in vacuo, diluted with water (20 mL), and extracted with CH_2Cl_2 (3 × 20 mL). The combined extracts were washed with water (3 × 20 mL), dried over Na_2SO_4, and concentrated in vacuo to yield a thick orange oil. Purification by silica gel flash chromatography (hexane/ethyl acetate, 10:1) afforded **16** as a yellowish liquid (2.55 g, 60%). ^{1}H NMR ($CDCl_3$): δ 1.53 (2H, p, J = 8.6 Hz, $-SeCH_2CH_2CH_2Se-$), 2.05 (4H, p, J = 8.6 Hz, $HSCH_2CH_2CH_2SeCH_2CH_2CH_2SeCH_2CH_2CH_2SH$), 2.88 (12H, p, J = 8.6 Hz, $HSCH_2CH_2CH_2SeCH_2CH_2-CH_2SeCH_2CH_2-CH_2SeCH_2CH_2SH$). ^{13}C NMR ($CDCl_3$): δ 22.1 (CH_2's α to Se, with triplet satellite peak), 23.7 (CH_2's α to Se, with triplet satellite peak), 24.4 (CH_2's β to SH), 31.1 (CH_2's β to Se), 34.3 (CH_2's α to SH). IR (neat): 2830−2940 (s, ν(CH)), 2540 (ν(SH)), 1440 (δ(CH)) cm^{-1}. MS: 350 ($M^{+\bullet}$). Anal. Calcd for $C_9H_{18}Se_2S_2$: C, 30.86; H, 5.71. Found: C, 30.92; H, 5.72.

16Se2S2 (3). A suspension of Cs_2CO_3 (2.0 g, 6.0 mmol) in dry DMF (50 mL) was heated to 60 °C. Dibromopropane (1.15 g, 6.0 mmol) in dry DMF (50 mL) and 1,3-bis((3-mercapto-1-propyl)selenio)propane (**16**) (2.0 g, 6.0 mmol) in DMF (50 mL) were added dropwise, from separate dropping funnels, to the above suspension over 3 h. The reaction mixture was stirred at 65−70 °C for 6 days. The solution was concentrated in vacuo, diluted with water (30 mL), and extracted with CH_2Cl_2 (3 × 30 mL). The combined extracts were washed with water (3 × 20 mL), dried over Na_2SO_4, and concentrated in vacuo to yield a thick orange oil. Purification by silica gel flash chromatography (hexane/ethyl acetate, 250:1.5) afforded **3** as white crystals (500 mg, 22%). Mp: 53−54 °C. ^{1}H NMR ($CDCl_3$): δ 1.97 (8H, 2p, J = 6.0 Hz, $-SCH_2CH_2CH_2S-$ and $-SeCH_2CH_2CH_2Se-$), 2.87 (8H t, J = 6.0 Hz, $-CH_2SeCH_2CH_2CH_2SeCH_2-$), 3.05 (8H, t, J = 6.0 Hz, $-CH_2SCH_2CH_2CH_2SCH_2-$). ^{13}C NMR ($CDCl_3$): δ 22.7 (CH_2's α to Se), 23.8 (CH_2's α to Se), 29.8 (β-CH_2's), 30.8 (β-CH_2's), 31.8, 32.0 (CH_2's α to S). IR (KBr): 2857, 2928 (s, ν(CH)), 1451 (s, δ(CH)), 1240, 1042 (ν(SeC) or ν(SC)) cm^{-1}. MS: 390 ($M^{+\bullet}$). Anal. Calcd for $C_{12}H_{24}Se_2S_2$: C, 36.92; H, 6.20. Found: C, 37.05; H, 6.27.

[Cu(16Se2S2)][SO$_3$CF$_3$]$_2$ (4). A solution of 16Se2S2 (**3**) (22 mg, 0.06 mmol) in dry acetone (0.5 mL) was added to $Cu(SO_3CF_3)_2$[49] (20 mg, 0.06 mmol) in dry acetone (0.5 mL). The mixture was cooled to 0 °C and stirred for 5 min. Vapor diffusion of diethyl ether into the solution resulted in the deposition of dark brown crystals, which were collected and washed with ether. The crystal for X-ray crystallography was prepared by diffusion of diethyl ether vapor into a solution of [Cu(16Se2S2)][SO_3CF_3]$_2$ in CH_3NO_2/CH_2Cl_2 (2:1, v/v) at ambient temperature. Dark brown, needle-shaped crystals were formed (20 mg, 47%). UV (CH_2Cl_2), λ_{max} (ϵ): 570 nm (900), 456 nm (6870), 280 nm (450). Anal. Calcd for $CuC_{14}H_{24}F_6O_6S_4Se_2$: C, 22.37; H, 3.20. Found: C, 22.49; H, 3.19.

[Cu(16Se4(OH)$_2$)][SO$_3$CF$_3$]$_2$ (5). A solution of 16Se4(OH)$_2$[11] (**9**) (14.3 mg, 0.03 mmol) in dry CH_2Cl_2 (1 mL) was added to $Cu(SO_3CF_3)_2$[49] (10 mg, 0.03 mmol) in dry CH_3NO_2 (2 mL). A dark brown solution was formed, which was stirred for 5 min at ambient temperature and then cooled to 0 °C. Diffusion of diethyl ether vapor into the brown solution yielded [Cu(16Se4(OH)$_2$)][SO_3CF_3]$_2$ (**5**) as dark brown crystals (12 mg, 49%). UV (CH_2Cl_2): λ_{max} (ϵ) 464 nm (11 900), 310 nm (2300). Anal. Calcd for $CuC_{14}H_{24}F_6O_8S_2Se_4$: C, 19.16; H, 2.70. Found: C, 19.34; H, 2.63.

[Cu(8Se2(OH)$_2$)][SO$_3$CF$_3$]$_2$ (6). A solution of $Cu(SO_3CF_3)_2$[49] (33 mg, 0.09 mmol) in CH_3NO_2 (2.5 mL) was added to a solution of 1,5-diselenacyclooctan-3-ol (8Se2(OH)[11] (**17**)) (46 mg, 0.18 mmol) in CH_3NO_2 (2.5 mL). The reaction mixture was stirred for 10 min at ambient temperature and then cooled to −10 °C. Filtration yielded **6** as dark brown crystals (45 mg, 61%). UV (CH_2Cl_2): λ_{max} (ϵ) 571 nm (8100), 510 nm (7050), 386 nm (7900). Anal. Calcd for $CuC_{14}H_{24}F_6O_8S_2Se_4$: C, 19.16; H, 2.76. Found: C, 19.36; H, 2.66.

[Cu(16Se2S$_2$)][SO$_3$CF$_3$] (7). Crystalline [Cu(16Se$_2$S$_2$)][SO_3CF_3]$_2$ (**4**) (15 mg) was dissolved in acetone (0.6 mL), and diethyl ether vapor was allowed to diffuse into the solution. After 24 h at ambient temperature, **7** was obtained as white, needle-shaped crystals. X-ray crystallography showed that the white crystals were the complex [Cu(16Se2S2)][SO_3CF_3] (**7**). Anal. Calcd for $CuC_{14}H_{24}F_6O_6S_4Se_2$: C, 25.91; H, 3.99. Found: C, 25.99; H, 4.01.

8Se2(SO$_3$CF$_3$)$_2$ (11). A solution of 1,5-diselenacyclooctane (8Se2)[9] (48 mg, 0.1 mmol) in dry acetone (0.5 mL) was added to $Cu(SO_3CF_3)_2$[49] (410 mg, 1.1 mmol) in dry CH_3CN and CH_2Cl_2 (0.5 mL, 2:1 v/v). The mixture was stirred for 5 min at ambient temperature and cooled to 3 °C overnight. The crystals were collected and recrystallized from CH_3CN to afford 8Se2(SO_3CF_3)$_2$ (**11**) as white crystals (234 mg, 49%). Mp: 167−168 °C dec. ^{1}H NMR (CD_3CN): δ 3.0−3.7 (4H, m, $SeCH_2CH_2CH_2Se$), 3.9−4.3 (8H, m, $CH_2SeCH_2CH_2CH_2SeCH_2$). ^{13}C NMR ($CDCl_3$): δ 36.1 (CH_2's β to Se), 52.3 (CH_2's α to Se). Anal. Calcd for $C_8H_{12}F_6O_6S_2Se_2$: C, 17.25; H, 2.22. Found: C, 17.53; H, 2.37.

[Cu(16Se4(OH))][SO$_3$CF$_3$]$_2$ (18). A solution of 16Se4(OH)[9] (**10**) (40 mg, 0.08 mmol) in dry acetone (0.5 mL) was added to $Cu(SO_3CF_3)_2$[49] (29 mg, 0.08 mmol) in dry acetone (0.5 mL). A dark brown solution was formed. Diffusion of diethyl ether vapor into the brown solution, overnight at 0 °C, yielded [Cu(16Se4(OH))][SO_3CF_3]$_2$ (**18**) as dark brown crystals. Anal. Calcd for $CuC_{14}H_{24}F_6O_7S_2Se_4$: C, 19.98;

(48) Clarembean, M.; Cravador, A.; Dumont, W.; Hevesi, L.; Krief, A.; Lucchette, T.; Van Ende, D. *Tetrahedron* **1985**, *41*, 4793.

(49) Denguchi, T. *J. Chem. Phys.* **1960**, *32*, 1584.

H, 2.82. Found: C, 19.51; H, 2.81. Attempted recrystallization in CH_3NO_2 with the diffusion of ether vapor yielded a mixture of the Cu(II) complex [Cu(16Se4(OH))][SO_3CF_3]$_2$ (**18**) as brown crystals and the Cu(I) complex [Cu(16Se4(OH))][SO_3CF_3] (**8**) as white crystals. Compound **8** was characterized by X-ray crystallography.

X-ray Crystallography. Complex scattering factors for neutral atoms[50] were used in the calculation of structure factors. The programs used for data reduction, structure solution, and graphical output were from the NRCVAX Crystal Structure System.[51] The program suite CRYSTALS[52] was employed in the refinement. Crystal and refinement data are shown in Table 1. All the structures involving the 1,5-diselena-9,13-dithiacyclohexadecane molecule or ligand (**3**, **4**, **7**) display disorder corresponding to the interchange of sulfur and selenium sites. Resolvable conformational disorder of some propanediyl subchains was modeled for **1**, **6**, **7**, and **8**. Orientational disorder of SO_3CF_3 groups was modeled in **4**, **5**, and **7**. Positional disorder for the hydroxyl substituent was modeled for **8**. Full details of the refinement strategies and results are included in the Supporting Information. Readers are advised to consult this material to better understand the significance of the results.

Results and Discussion

1. Synthesis, Redox Behavior, and NMR Spectroscopic Studies. (A) Selenium Coronands. (i) Synthesis. Dibenzo-14Se4 (**1**) was synthesized in a stepwise manner, as shown in Scheme 1. Reduction of poly(1,2-diseleniobenzene) (**12**)[47] with $NaBH_4$ afforded sodium 1,2-benzenediselenolate, which was reacted with 3-bromo-1-propanol to give 1,2-bis((3-hydroxy-1-propyl)selenio)benzene (**13**). The diol was transformed into the dichloride **14** by reaction with thionyl chloride. Reaction of **14** with sodium 1,2-benzenediselenolate afforded the target coronand 6,7,13,14-dibenzo-1,5,8,12-tetraselenacyclotetradecane (**1**).

Extension of the synthetic approach to the synthesis of analogues containing only two-carbon bridges by reaction of sodium 1,2-benzenediselenolate with 1,2-bis((3-halo-1-ethyl)-selenio)benzene was not successful due to the formation of labile ethylene episelenonium ions which decomposed by extrusion of ethylene.[53−55]

A stepwise synthesis of 16Se2S2 (**3**) was performed in a manner analogous to that used for the thiamacrocycles.[56] Treatment of 1,3-propanediyldiselenium dicyanide (**15**)[48] with $NaBH_4$ followed by 3-chloro-1-propanethiol afforded 5,9-diselenatridecane-1,13-dithiol (**16**) (Scheme 2). Cyclization with 1,3-dibromopropane was achieved in the presence of Cs_2CO_3 to afford the desired coronand, 1,5-diselena-9,13-dithiacyclohexadecane (**3**).

(ii) Solid-State NMR Studies. Compounds **2**, **3**, **9**,[11] **10**,[11] and **11** were examined by solid-state ^{13}C and ^{77}Se NMR spectroscopy. The isotropic shifts are collected in Table 2. The ^{13}C shifts are generally unexceptional. For the neutral compounds, ^{77}Se shifts are in the range characteristic of dialkyl selenides,[57] as might be expected. The dicationic compounds **11** and 16Se4(SO_3CF_3)$_2$[16] resonate at lower field, as would be expected for compounds based on Se^+. The downfield shifts are larger than those typical of R_3Se^+ in solution[57] and perhaps contain a contribution from the transannular Se−Se bonds present in these ions.[16,58,59]

In the cases of 16Se4(OH) (**10**) and 8Se2(SO_3CF_3)$_2$ (**11**), we have determined the chemical shift anisotropy from spinning sideband intensities,[60] and the principal components of the chemical shifts are reported in Table 3. It is interesting to note that the ^{77}Se shift tensor for **11** is axially symmetric, within experimental error. This is not required by crystal symmetry;[59] possibly it arises from one principal direction lying along the Se−Se bond. The C−Se bonds are nearly perpendicular to the Se−Se bond, and the principal values lying in the perpendicular plane might well be nearly equal.

(iii) Cyclic Voltammetry. (a) Dibenzo-14Se4 (1). Coronand **1** showed an irreversible cyclic voltammogram. The potential was scanned from 0 V, at 20 mV/s, vs SCE toward the anodic direction and back again. A single peak was observed at 0.9 V, and no cathodic peak was observed. As the scan rate was increased, the anodic peak potential shifted toward the more anodic direction. A plot of the anodic peak current versus the square root of the scan rate was a straight line, indicating that the oxidation process was diffusion controlled.

(b) 12Se3 (2). The cyclic voltammogram of **2** suggested that the oxidation process involved two consecutive one-electron-transfer steps. Over a scanning potential range of 0 to 1.65 V vs SCE, two waves were observed ($E_{1/2}$ = 0.52 and 1.63 V at a scan rate of 20 mV/s). These two waves correspond to the following two reactions:

$$12Se3 - e \rightarrow 12Se3^{+\bullet}$$

$$12Se3^{+\bullet} - e \rightarrow 12Se3^{2+}$$

However, the second reduction ($12Se3^{2+}/12Se3^{+\bullet}$) process became irreversible, even when the scan rate was 50 mV/s, as evidenced by the disappearance of the second cathodic peak on the reverse scan. Plots of the first and second anodic peak currents versus the square root of the scan rate were straight lines, indicating that the oxidation processes were diffusion controlled.

(c) 16Se2S2 (3). The cyclic voltammogram of **3**, recorded with a platinum electrode in MeCN (0.1 M Et_4NClO_4) at a scan rate of 100 mV/s, gave an anodic peak at 1.0 V vs SCE. The cathodic peak was observed at 0.11 V on the reverse scan ($E_{1/2}$ = 0.54). The separation of the potential peaks (ΔE_p) was 0.85 V, indicating that the electrode reaction was quasi-reversible. When the scan rate was increased, an increase in the potential peak separation was observed. When the scan rates were lower than 100 mV/s, the cathodic peak on the reverse scan disappeared. This suggested that the oxidized species of 16Se2S2 (**3**) in solution underwent homogeneous reactions, which resulted in electrochemically inactive species within the potential scan ranges. A plot of the anodic peak current versus the square root of the scan rate was a straight line, indicating that the oxidation of 16Se2S2 (**3**) was a diffusion-controlled electrode process. Controlled-potential electrolysis experiments performed on the coronand 16Se2S2 (**3**) in MeCN yielded yellow solutions.

(50) *International Tables for X-ray Crystallography*; Kynoch Press: Birmingham, England, 1975, Vol. IV, p 99.
(51) Gabe, E. J.; LePage, Y.; Charland, J.-P.; Lee, F. L.; White, P. S. NRCVAX−An Interactive Program System for Structure Analysis. *J. Appl. Crystallogr.* **1989**, *22*, 384.
(52) Watkin, D. J.; Carruthers, J. R.; Betteridge, P. W. *CRYSTALS*; Chemical Crystallography Laboratory, University of Oxford: Oxford, England, 1984.
(53) Lindgren, B. *Acta Chem. Scand., Ser. B* **1977**, *31*, 1.
(54) Lindgren, B. *Tetrahedron Lett.* **1974**, 4347.
(55) Lindgren, B. *Acta Chem. Scand., Ser. B* **1976**, *30*, 941.
(56) Ochrymowycz, L. A.; Mak, C.; Michna, J. D. *J. Org. Chem.* **1974**, *39*, 2079.
(57) Rodger, C.; Sheppard, N.; McFarlane, C.; McFarlane, W. In *NMR and the Periodic Table*; Harris, R. K., Mann, B. E., Eds.; Academic Press: New York, 1978; p 383.
(58) Furukawa, N.; Fujihara, H.; Akaishi, R.; Iwasaki, F.; Toyoda, M. *Bull. Chem. Soc. Jpn.* **1988**, *61*, 2563.
(59) Iwasaki, F.; Morimoto, M.; Yasui, M.; Akaishi, R.; Fujihara, H.; Furukawa, N. *Acta Crystallogr., Sect. C* **1991**, *47*, 1463.
(60) Herzfeld, J.; Berger, A. *J. Chem. Phys.* **1980**, *73*, 6021.

Table 1. Crystallographic Data for the Structure Determinations of 6,7,13,14-Dibenzo-1,5,8,12-tetraselenacyclotetradecane (**1**), 1,5,9-Triselenacyclododecane (**2**), 1,5-Diselena-9,13-dithiacyclohexadecane (**3** = 16Se2S2), [Cu(16Se2S2)][SO_3CF_3]$_2$ (**4**), [Cu(16Se4(OH))$_2$][SO_3CF_3]$_2$ (**5**), [Cu(8Se2(OH))$_2$][SO_3CF_3]$_2$ (**6**), [Cu(16Se2S2)][SO_3CF_3] (**7**), and [Cu(16Se4(OH))][SO_3CF_3] (**8**)

	1[a,b]	**2**[a,c]	**3**[a,d]	**4**[a,e]	**5**[f,h]	**6**[f,h]	**7**[a,i]	**8**[a,g]
empirical formula	$Se_4C_{18}H_{20}$	$Se_3C_9H_{18}$	$Se_2S_2C_{12}H_{24}$	$Se_2CuS_4F_6O_6C_{14}H_{24}$	$Se_4CuS_2F_6O_8C_{14}H_{24}$	$Se_4CuS_2F_6O_8C_{14}H_{24}$	$Se_2CuS_3F_3O_3C_{13}H_{24}$	$Se_4CuSF_3O_4C_{13}H_{24}$
cryst syst	orthorhombic	orthorhombic	monoclinic	monoclinic	monoclinic	monoclinic	triclinic	monoclinic
fw	552.19	363.12	390.36	752.03	877.84	877.84	602.97	712.77
space group	$Pca2_1$	$Pn2_1a$	$C2/c$	$P2_1/n$	$P2_1/n$	$P2_1/c$	$P\bar{1}$	$P2_1/n$
a (Å)	9.645(3)	14.943(4)	24.202(9)	8.882(2)	8.412(5)	6.875(2)	10.512(3)	13.695(2)
b (Å)	12.679(6)	5.638(2)	18.005(7)	10.874(2)	20.924(5)	10.945(2)	10.674(2)	11.202(2)
c (Å)	15.332(4)	14.229(3)	16.235(5)	13.360(2)	15.021(5)	17.496(2)	10.682(3)	14.163(3)
α (deg)							101.47(2)	
β (deg)			138.23(3)	97.95(2)	100.82(4)	96.76(2)	116.82(2)	92.35(2)
γ (deg)							93.59(2)	
T (K)	190	190	200	297	190	195	205	297
V (Å^3)	1874.9	1198.8	4713	1277.9	2597	1307.3	1032.3	2170.9
Z	4	4	12	2	4	2	2	4
ρ_c (g cm^{-3})	1.956	2.012	1.651	1.954	2.245	2.230	1.940	2.181
λ(Mo Kα_1) (Å)	0.709 30	0.709 30	0.709 30	0.709 30	0.709 30	0.709 30	0.709 30	0.709 30
μ(Mo Kα) (cm^{-1})	77.4	90.7	48.9	40.6	66.3	65.8	48.8	77.8
cryst dimens (mm)	0.17 × 0.21 × 0.24	0.14 × 0.20 × 0.28	0.19 × 0.27 × 0.28	0.10 × 0.16 × 0.24	0.14 × 0.16 × 0.40	0.21 × 0.28 × 0.29	0.05 × 0.14 × 0.32	0.06 × 0.18 × 0.19
transmn	0.271−0.346[j]	0.191−0.332[j]	0.318−0.490[j]	0.564−0.664[j]	0.337−0.475[j]	0.873−1.000 (rel)[k]	0.537−0.767[j]	0.370−0.645[j]
2θ range (deg)	4−54	4−50	4−45	4−50	4−45	4−50	4−46	4−45
no. of reflns ($I_o \geq 2.5\sigma(I_o)$)	1732	862	1881	2232	2152	1816	2237	2086
R_F[l]	0.027	0.026	0.052	0.028	0.059	0.023	0.029	0.035
R_{wF}[m]	0.026[n]	0.027[n]	0.062[o]	0.032[p]	0.061[o]	0.025[q]	0.037[r]	0.036[o]

[a] Cell dimensions were determined from 25 reflections. [b] 32° ≤ 2θ ≤ 41°. [c] 34° ≤ 2θ ≤ 46°. [d] 32.7° ≤ 2θ ≤ 41.2°. [e] 32.0° ≤ 2θ ≤ 41.5°. [f] Cell dimensions were determined from 24 reflections. [g] 30° ≤ 2θ ≤ 40°. [h] 35° ≤ 2θ ≤ 40°. [i] 30° ≤ 2θ ≤ 45°. [j] The data were corrected by the Gaussian integration method for the effects of absorption. [k] The data were corrected empirically (ψ scan) for the effects of absorption. [l] $R_F = \sum||F_o| - |F_c||/\sum|F_o|$. [m] $R_{wF} = [\sum w(|F_o| - |F_c|)^2/\sum wF_o^2]^{1/2}$. [n] $w = [\sigma(F_o^2) + 0.0001F_o^2]^{-1}$. [o] Unit weights. [p] $w = [\sigma(F_o^2) + 0.0002F_o^2]^{-1}$. [q] $w = [32.974t_0(x) + 43.084t_1(x) + 20.289t_2(x)]^{-1}$; $x = |F_o|/F_{max}$ and t_n are the polynomial functions of the Chebyshev series: Carruthers, J. R.; Watkin, D. J. *Acta Crystallogr*. **1979**, *A35*, 698. [r] $w = [\sigma(F_o^2) + 0.0003F_o^2]^{-1}$.

Scheme 1

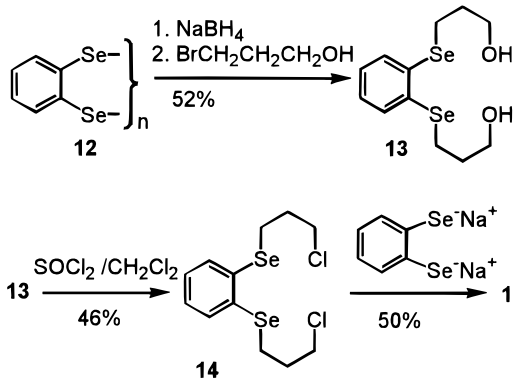

Scheme 2

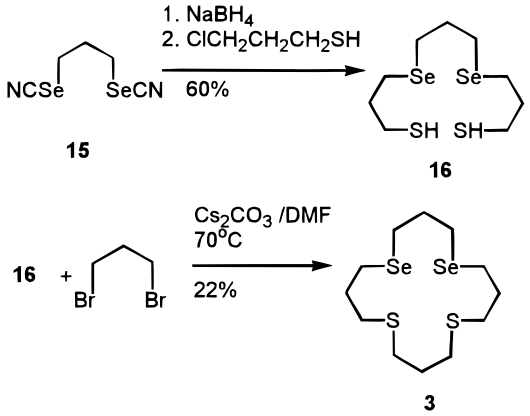

Table 2. Solid-State CP-MAS ^{77}Se NMR and ^{13}C NMR Spectroscopic Data

compd	δ (rel int) ^{77}Se[a]	^{13}C[b]
12S3	300	35.1 (1)
2	206	26.8 (1)
16Se2S2	199 (1)	19−22 (1) (unresolved)
3	179 (1)	26−34 (3) (unresolved)
	136 (1)	
16Se4(OH)$_2$	192 (1)	76 (1)
9	155, 145, 134 (2)	37 (2), 34 (2), 29 (1.5)
	113 (1)	
16Se4(OH)	167 (1)	71.7 (1)
10	131 (1)	33.3, 33.0 (3)
		28.7 (1)
8Se2(SO$_3$CF$_3$)$_2$	810 (1)	52.7 (3)
11	768 (1)	34.5 (2)
		120 (1)
		121

[a] In ppm relative to Me_2Se. [b] In ppm relative to TMS.

Although only one pair of redox waves was observed in the cyclic voltammogram, the amount of charge passed through the solution indicated an overall two-electron process.

(iv) Chemical Generation of Radical Cations. Radical cations of the selenium coronands were produced by injecting an $NOBF_4$ solution into a deoxygenated solution of the coronand, being stirred in a UV cell. Recording of UV−visible spectra was commenced as soon as the $NOBF_4$ solution was added. The UV spectroscopic scanning was repeated at intervals based on the selenium coronand. The formation of the corresponding selenium coronand radical cation was indicated by the appearance of a characteristic absorption. The intensity of the absorption increased rapidly in about 2 min after the addition of $NOBF_4$, and after 2 min, the growth slowed substantially. Upon mixing with $NOBF_4$ (4.0×10^{-5} M), 12Se3 (**2**) (1.3×10^{-4} M) and 16Se2S2 (**3**) (1.3×10^{-4} M) yielded yellow solutions with absorbances at 282 and 300 nm, respectively. The species were attributed to the corresponding radical cations.[16] Coronand dibenzo-14Se4 (**1**) was apparently not oxidized by $NOBF_4$, since no color change or new absorption peaks were observed.

Table 3. Chemical Shift Anisotropies for 16Se4(OH) (**10**) and 8Se2(SO$_3$CF$_3$)$_2$ (**11**)

10		**11**	
isotropic shift[a]	principal components[a]	isotropic shift[a]	principal components[a]
167	299 ± 6	810	1066 ± 6
	132 ± 7		1066 ± 6
	70 ± 5		300 ± 10
131	264 ± 10	768	1005 ± 5
	83 ± 13		1005 ± 5
	47 ± 9		292 ± 10

[a] In ppm relative to Me_2Se.

(B) Cu Complexes. (i) Synthesis. (a) The Cu(I) and Cu(II) Complexes of 16Se2S2 (3). The complex (1,5-diselena-9,13-dithiacyclohexadecane)copper(II) trifluoromethanesulfonate (**4**) was synthesized by the addition of 16Se2S2 (**3**) in acetone to a solution of Cu(SO$_3$CF$_3$)$_2$ in acetone. From the dark brown solution were isolated brown crystals, which were recrystallized from CH_3NO_2 with diethyl ether vapor diffusion into the solution. The spontaneous reduction of [Cu(16Se2S2)][SO$_3$CF$_3$]$_2$ (**4**) in organic solvents was observed during recrystallization. To obtain crystals for X-ray crystallography, several solvent systems were attempted. From CH_3NO_2/CH_2Cl_2 (2:1, v/v) with ether vapor diffusion were isolated crystals of **4** of reasonable quality for X-ray crystallography. However, from the acetone solution with ether vapor diffusion were obtained white crystals that were identified as being [Cu(16Se2S2)][SO$_3$CF$_3$] (**7**) by microanalysis and X-ray crystallography.

The redox process that produced **7** was also monitored by UV−visible spectroscopy. The brown CH_2Cl_2 solution of **4** showed one absorption band above 250 nm: λ_{max} 456 nm (ϵ 6870) with shoulders at 570 nm (ϵ 900) and 280 nm (ϵ 450). Addition of ligand **3** to the Cu(II) complex **4** in CH_2Cl_2 caused the absorption peak at 464 nm to decrease and a new peak at 310 nm to appear. The peak at 310 nm was attributed to the absorption of the radical cation of **3**, which was confirmed by the reaction of $NOBF_4$ with **3** in CH_3CN. This behavior is analogous to that observed with the Cu(II) complex of 16Se4 upon addition of free 16Se4.[12,16] The formation of **7** may be represented by the following redox reaction:

$$\underset{\mathbf{4}}{[Cu(16Se2S2)]^{2+}} + \underset{\mathbf{3}}{16Se2S2} \rightarrow \underset{\mathbf{7}}{[Cu(16Se2S2)]^{+}} + \underset{\mathbf{3}^{+\bullet}}{16Se2S2^{+\bullet}}$$

(b) The Cu(II) Complex of 16Se4(OH)$_2$ (9).[11] The complex (1,5,9,13-tetraselenacyclohexadecane-3,11-diol)copper(II) trifluoromethanesulfonate, [Cu(16Se4(OH)$_2$)][SO$_3$CF$_3$]$_2$ (**5**), was synthesized by the addition of 16Se4(OH)$_2$ (**9**)[11] in CH_2Cl_2 to a solution of Cu(SO$_3$CF$_3$)$_2$ in CH_3NO_2. From the dark brown solution were isolated brown crystals after diethyl ether vapor diffusion into the solution.

(c) The Cu(II) Complex of 8Se2(OH) (17).[11] The complex bis(1,5-diselenacyclooctan-3-ol)copper(II) trifluoromethanesulfonate, $[Cu(8Se2(OH))_2][SO_3CF_3]_2$ (**6**), was synthesized by the addition of 8Se2(OH) (**17**)[11] in CH_3NO_2 to a solution of $Cu(SO_3CF_3)_2$ in CH_3NO_2. Dark brown crystals were isolated.

(d) The Cu(II) and Cu(I) Complexes of 16Se4(OH) (10).[11] The complex (1,5,9,13-tetraselenacyclohexadecan-3-ol)copper-(II) trifluoromethanesulfonate, $[Cu(16Se4(OH))][SO_3CF_3]_2$ (**18**), was synthesized by the addition of 16Se4(OH) (**10**)[11] in acetone to a solution of $Cu(SO_3CF_3)_2$ in acetone. Dark brown crystals were isolated. These crystals were found to be unstable in CH_3NO_2 when ether vapor was diffused into the solution. A mixture of the Cu(II) complex **18** (brown crystals) and Cu(I) complex $[Cu(16Se4(OH))][SO_3CF_3]$ (**8**) (white crystals) was obtained.

(e) The Cu(II) Complex of Dibenzo-14Se4 (1). The preparation of this complex was not successful. When an acetone solution of dibenzo-14Se4 (**1**) was mixed with an acetone solution of $Cu(SO_3CF_3)_2$, a dark brown solution was formed immediately, which discolored to a greenish solution upon standing. With the diffusion of ether into the above solution, colorless crystals precipitated, which were identified as being the starting ligand **1**.

(ii) Cyclic Voltammetry. (a) $[Cu(16Se2S2)][SO_3CF_3]_2$ (4). The cyclic voltammogram of **4** was recorded in CH_2Cl_2 (with 0.05 M TEAP as supporting electrolyte) at a Pt working electrode. Over a potential scanning sweep from 1.2 to 0 V and then back to 1.2 V, a pair of quasi-reversible redox waves was observed ($E_{1/2} = 0.72$ V, $\Delta E_p = 0.27$ V, half potential peak width ($E_p - E_{p/2}$) = 0.11 V, and $i_a/i_c = 0.94$ at a scan rate 20 mV/s). An increase in the scan rates resulted in an increase in the potential peak separation (ΔE_p) between the anodic peak and the cathodic peak, which suggested that the electrode process was a quasi-reversible one-electron-transfer redox reaction; the reaction was attributed to the redox couple $Cu^{II}L/Cu^{I}L$.

When the potential was scanned from 0 to 1.2 V and then back to 0 V, at a scan rate of 20 mV/s, a pair of quasi-reversible redox waves was observed ($E_{1/2} = 0.77$ V vs SCE; $\Delta E_p = 0.12$ V, $E_p - E_{p/2} = 0.09$ V). The ratio of i_a/i_c was 0.78. These parameters suggested a faster electrode reaction when the initial potential started at 0 V, at which point **4** was reduced to $[Cu(16Se2S2)][SO_3CF_3]$ (**7**) in the vicinity of the Pt electrode.

When the potential was scanned (50 mV/s) from 1.0 V toward 1.8 V, **4** was oxidized further, resulting in an anodic peak at 1.43 V, but no cathodic peak appeared on the reverse scan. When the scan rate was increased to 500 mV/s, the cathodic peak on the reverse scan was observed at 1.22 V with an i_a/i_c ratio of 0.14, implying that there are complications due to homogeneous chemical reactions that consume the oxidized $Cu^{II}L$ species and compete with the electrode reaction. When the scan rate was 20 mV/s, the anodic current did not form a peak; instead a plateau appeared.

The dependence of the cyclic voltammograms of $[Cu(16Se2S2)][SO_3CF_3]$ (**4**) on the initial-scan potentials may result from different conformational species; the E_{pa} values from the cyclic voltammograms of scan range 0−1.2 V are lower than those from the cyclic voltammograms of scan range 1.2−0 V. We propose that, at the initial potential of 0 V, $[Cu(16Se2S2)][SO_3CF_3]$ is transformed into a more reactive species (**B**) through an equilibrium reaction with the less reactive species (**A**), as shown in Scheme 3; hence, the oxidation peak appears at lower potential. On the other hand, in the scan range from 1.2 to 0 V, the reduced species has less time to equilibrate to the more reactive species and the oxidation peak appears at a higher potential.

Scheme 3

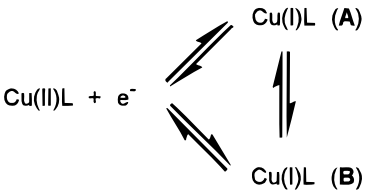

The redox wave at 1.1 V vs SCE may be attributed either to the oxidation of the selenium coronands in the complexes or to the oxidation of Cu(II) complexes to Cu(III) complexes. The reported Cu(III) complexes of a nitrogen coronand (14N4)[61] and of other nitrogen-containing ligands (peptides),[62−68] obtained from the oxidation of Cu(II) complexes of the corresponding ligands, have redox potentials of 1.0 V vs SCE.[63,65,66]

(b) $[Cu(16Se4(OH)_2)][SO_3CF_3]_2$ (5). The cyclic voltammogram of **5**, recorded in CH_3NO_2 (with 0.1 M TEAP as supporting electrolyte), with a potential scanning sweep from −0.4 to +1.0 V and back to −0.4 V, showed a broad anodic peak at 0.69 V and a cathodic current peak at 0.43 V ($E_{1/2} = 0.52$ V, $\Delta E_p = 154$ mV, and $i_a/i_c = 0.46$; at a scan rate of 20 mV/s). These redox waves correspond to a quasi-reversible one-electron electrode reaction of the $Cu^{II}L/Cu^{I}L$ pair. The separation between the anodic and cathodic peaks was scan rate dependent; the peak separation ΔE_p increased as the scan rates increased, but the anodic to cathodic current ratios decreased.

At a scan rate of 50 mV/s, the broad anodic current peak was composed of two peaks with maxima at 0.65 and 0.77 V. The latter increased in intensity as the scan rate increased, and eventually the two peaks merged to one peak (0.80 V) at a scan rate of 200 mV/s. This indicates the presence of different isomers of the Cu(I) species, which were oxidized at different potentials. At slow scanning rates, mainly the less stable species (**B**) was oxidized (Scheme 3). When the scanning rates exceeded the **A** to **B** conversion rate, the oxidation of the more stable isomer (**A**) dominated and only one oxidation peak was observed at the higher potential. A small peak at 0.26 V in the anodic scan at scan rates over 100 mV/s was also observed. When the anodic potential exceeded 1.4 V, **5** was oxidized further and a second oxidation peak was seen ($E_{1/2} = 0.72$ V). This may be due to the Cu(III) species or due to the Cu(II) species with further oxidation of the ligand.

(c) $[Cu(8Se2(OH)_2)][SO_3CF_3]_2$ (6). The cyclic voltammogram of **6** was recorded in CH_3NO_2 (with 0.1 M TEAP as the supporting electrolyte) with a carbon electrode as the working electrode (the reaction was sluggish on a platinum electrode). Over a potential sweep loop from +0.8 to −0.4 V and then to

(61) Fabbrizzi, L.; Castellani, C. B.; Licchelli, M.; Perotti, A.; Poggi, A. *J. Chem. Soc., Chem. Commun.* **1984**, 806.
(62) Sayre, L. M.; Reddy, K. V.; Jin, S.; Arora, P. K.; Sfeir, D. S.; Maloney, S. C. F.; Urbach, F. L. *J. Am. Chem. Soc.* **1990**, *112*, 2332.
(63) Margerum, D. W.; Chellappa, K. L.; Basu, F. P.; Burce, G. L. *J. Am. Chem. Soc.* **1975**, *97*, 6894.
(64) Margerum, D. W.; Bossu, F. P.; Chellappa, K. L. *J. Am. Chem. Soc.* **1977**, *99*, 2195.
(65) Margerum, D. W.; Neubecker, T. A.; Kirksey, J. S. T.; Chellappa, K. L. *Inorg. Chem.* **1979**, *18*, 444.
(66) Margerum, D. W.; Rybka, J. S.; Kurtz, J. L.; Neubecker, T. A. *Inorg. Chem.* **1980**, *19*, 2791.
(67) Steggerda, J. J.; Bour, J. J.; Birker, P. J. M. W. L. *Inorg. Chem.* **1971**, *10*, 1202.
(68) Collins, T. J.; Anson, F. C.; Richmond, T. G.; Santarsiero, B. D.; Toth, J. E.; Treco, B. G. R. T. *J. Am. Chem. Soc.* **1987**, *109*, 2974.

1.2 V, a quasi-reversible cyclic voltammogram was observed. A cathodic peak at 0.39 V and a broad anodic peak centered at 0.68 V, corresponding to the single-electron-transfer redox couple $Cu^{II}L/Cu^{I}L$ ($E_{1/2} = 0.53$ V vs SCE at a scan rate of 20 mV/s, $\Delta E_p = 0.28$ V, $i_a/i_c = 0.74$), were observed. The broad oxidation peaks indicate the presence of different isomers of the Cu(I) species, which are oxidized at different potentials, as described above for **5**. When the scan rate was increased, the anodic/cathodic peak current ratio increased. The same cyclic voltammogram was obtained with a scan loop from 0 to 1.4 V and then back to 0 V. Furthermore, scanning the potential up to 1.6 V did not give a second oxidation peak, as observed for the previous Cu(II) complexes of selenium coronands.

(iii) Controlled-Potential Electrolysis. Controlled-potential electrolysis experiments were performed on $[Cu(16Se2S2)][SO_3CF_3]_2$ (**4**) and $[Cu(16Se4(OH)_2)][SO_3CF_3]_2$ (**5**) (0.05 M in CH_2Cl_2 with TEAP as supporting electrolyte) in a two-compartment cell on a Pt electrode. At the applied potential of 0 V vs SCE, electrolysis occurred, as manifested by a change in the brown solution to a light yellow solution. The total electric charge passed through the solution, recorded on a coulometer, indicated that the reduction was a one-electron process for each complex.

(iv) Redox Behavior. Cyclic voltammetry of the Cu(II) complexes of selenium coronands has shown that the redox reaction of the $Cu^{II}L/Cu^{I}L$ pair is chemically reversible. This reversibility may result from the stabilization of Cu(I) ions through coordination to the selenium coronands. The usual oxidation states of copper are Cu(II) and Cu(I). In aqueous solution, the Cu(II) ion is more stable than Cu(I) because Cu(II) has a higher heat of hydration, whereas Cu(I) undergoes a disproportionation reaction.[69] Therefore, no anodic peaks are observed on the reverse scans in the cyclic voltammograms of aqueous solutions of Cu(II).

Another indication of the stabilization of the Cu(I) ion by the coordination environment around the Cu atom is that the redox potential of Cu(II) rises in complexes of selenium coronands; the $E_{1/2}$ values are in the range 0.4−0.8 V vs SCE in contrast to those of Cu(II) complexes with nitrogen- or oxygen-donor ligands whose $E_{1/2}$ values are between 0 and −0.7 V vs SCE in aqueous solution.[36,70]

Similarly, increased redox potentials have also been observed for the Cu(II) complexes of thia macrocycles (∼0.7 V vs NHE).[71] Two factors have been proposed to explain the unusual redox potentials of Cu(II) complexes of thia macrocycles: (1) The Cu(I) ions are stabilized by the stereochemical properties of the ligands, which alter the properties of Cu(II) ions by constricting and dilating their coordination spheres.[72] Patterson and Holm[70] have shown that structural factors which facilitate configuration changes (from tetragonal to tetrahedral configurations) of complexes result in high redox potentials, for a series of bis(chelate) amine Cu(II) complexes. (2) The electronic properties of thioethers lead to $d\pi-d\pi$ interactions between ligands and Cu atoms, resulting in delocalization of the electron density from the filled Cu(I) 3d orbitals into empty sulfur 3d orbitals;[36] a similar explanation has been proposed for the ability of phosphines to stabilize the low-valence states of transition metal ions.[73−76] Molecular orbital calculations suggest that $d\pi-d\pi$ interactions (π-acidity) make a greater contribution to the stabilization of Cu(I)−thioether complexes than to that of Cu(II)−thioether complexes.[75] A recent calculation indicates that dimethyl selenoether has weak π-acidity.[77]

The conformations of the selenium coronands in the Cu(II) complexes are quite different from those of the free ligands. The constraints imposed on the Cu(II) ion in the complexes may result in high redox potentials. The spontaneous reduction of the Cu(II) selenium coronand complexes to Cu(I) selenium coronand complexes indicates the preferential stabilization of Cu(I) ions by the selenium coronands.

The configurational changes between copper(II) complexes (octahedral or tetragonal configurations)[78] and Cu(I) complexes (tetrahedral configurations) may be reflected in the cyclic voltammograms of the Cu(II)−selenium coronand complexes. A reversible cyclic voltammogram corresponds to a system in which the electron transfer to the electrode is the rate-determining step;[79] i.e., the configuration change of a complex must be faster than the electron transfer. Otherwise, quasi-reversible or even irreversible cyclic voltammograms would be produced. The quasi-reversible cyclic voltammograms observed for the copper(II) complexes of selenium coronands suggest that the configuration changes were slower than the electron transfers to the electrodes.

The cyclic voltammetry results for complexes **4**, **5**, and **6** are consistent with Scheme 3, which indicates the presence of two different conformational isomers of the Cu(I) species, **A** and **B**, that are oxidized at different potentials. Our system is analogous to that of Rorabacher's Cu(II/I) complexes of macrocyclic tetrathiaether ligands, in which the electron-transfer reactions follow a dual-pathway square scheme mechanism; here, conformational changes and electron-transfer steps occur sequentially, rather than concertedly.[80,81] Under conditions where a conformational change is the rate-limiting process, the electron transfer is referred to as gated electron transfer.[82] Under these conditions, the rate of electron transfer is limited in only one direction.[83]

2. X-ray Crystallographic Studies of the Selenium Coronands and Cu Complexes. The crystal structure of **1** presents a disordered superposition of two conformers. The molecular structure of the predominant (67.0(7)%) solid-state conformation of **1** is shown in Figure 2a. A second conformation (33.0(7)%), shown in Figure 2b, replaces the chain C(5)−C(6)−C(7)−Se(8) with C(15)−C(16)−C(17)−Se(18). Selected bond distances, bond angles, and torsion angles for **1** are given in the Supporting Information. Differences in the lengths of chemically equivalent bonds involved in the disorder are not considered to be significant. The previously noted tendency for C−Se−C−C sequences to adopt gauche torsional arrangements[9] is exemplified by these conformers. The minor conformer differs primarily

(69) McAuley, A. *Coord. Chem. Rev.* **1970**, *5*, 245.
(70) Patterson, G. S.; Holm, R. H. *Bioinorg. Chem.* **1975**, *4*, 257.
(71) Rorabacher, D. B.; Dockal, E. R.; Jones, T. E.; Sokol, W. F.; Engerer, R. J.; Ochrymowycz, L. A. *J. Am. Chem. Soc.* **1976**, *98*, 4322.
(72) Cooper, S. R.; Rawle, S. C. *Struct. Bonding* (*Berlin*) **1990**, *72*, 1.
(73) Taube, H.; Scott, N. S. *Inorg. Chem.* **1981**, *20*, 3135.
(74) Mitchell, K. A. R. *Chem. Rev.* **1969**, *69*, 157.
(75) Nikles, D. E.; Anderson, A. B.; Urbach, F. L. In *Copper Coordination Chemistry: Biochemical and Inorganic Perspectives*; Karlin, K. D., Zubieta, J., Eds.; Adenine Press: Guilderland, New York, 1983; p 203.
(76) Cotton, F. A.; Wilkinson, G. *Advanced Inorganic Chemistry*, 4th ed.; John Wiley & Sons: New York, 1980; p 799.
(77) Kraatz, H.; Jacobsen, H.; Ziegler, T.; Boorman, P. M. *Organometallics* **1993**, *12*, 76.
(78) Hathaway, B. J.; Billing, D. E. *Coord. Chem. Rev.* **1970**, *5*, 143.
(79) Musker, W. K.; Olmstead, M. M.; Kessler, R. M. *Inorg. Chem.* **1984**, *23*, 3266.
(80) Villeneuve, N. M.; Schroeder, R. R.; Ochrymowycz, L. A.; Rorabacher, D. B. *Inorg. Chem.* **1997**, *36*, 4475.
(81) Salhi, C. A.; Qiuyue, Y.; Heeg, M. J.; Villeneuve, N. M.; Juntunen, K. L.; Schroeder, R. R.; Ochrymowycz, L. A.; Rorabacher, D. B. *Inorg. Chem.* **1995**, *34*, 6053.
(82) Hoffman, B. M.; Ratner, M. A. *J. Am. Chem. Soc.* **1987**, *109*, 6237.
(83) Brunschwig, B. S.; Sutin, N. *J. Am. Chem. Soc.* **1989**, *111*, 7454.

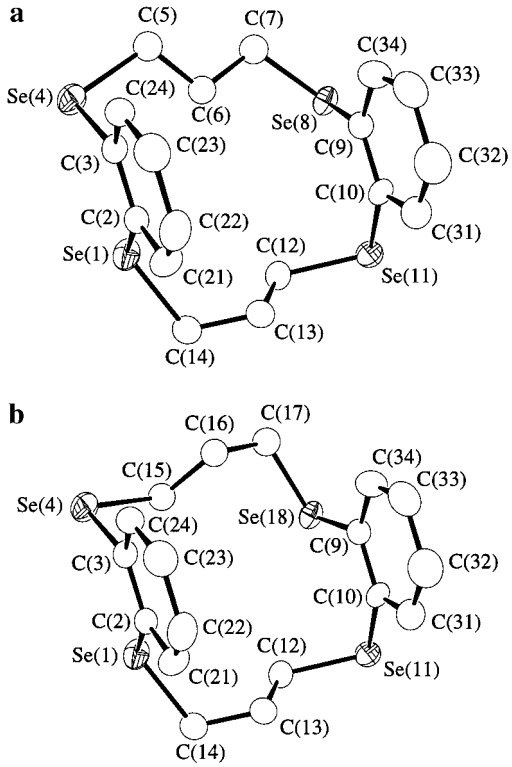

Figure 2. Molecular structures of the major conformer (a) and minor conformer (b) of **1**. 50%-enclosure thermal ellipsoids or spheres for the non-hydrogen atoms are shown.

from the major in that C(15)−C(16)−C(17) is pivoted away from the C(5)−C(6)−C(7) positions, about an axis passing through Se(4), while the anti torsional arrangement for Se(4)−C(5)−C(6)−C(7) (175.0(8)°) is essentially retained in Se(4)−C(15)−C(16)−C(17) (−174.9(13)°). This involves major conformational changes in two bond torsion angles. The positive gauche arrangement, C(3)−Se(4)−C(5)−C(6) 63.9(4)°, changes to the negative gauche arrangement, C(3)−Se(4)−C(15)−C(16) −65.2(7)°, while the approximately anti arrangement, C(5)−C(6)−C(7)−Se(8) 169.8(8)°, becomes the negative gauche arrangement, C(15)−C(16)−C(17)−Se(18) −64.4(9)°. Rationale for the occurrence of two such conformers of similar energies may be found in the following observations. The minor (33.0(7)%) conformer displays approximate 2-fold symmetry for the molecule but has two nearly eclipsed arrangements: C(14)−Se(1)−C(2)−C(21) −18.2(4)° and C(17)−Se(18)−C(9)−C(34) −18.6(5)°. These are associated with the most severe "unimposed" intramolecular contacts (i.e., C(17)- -C(34) 3.054(18) Å and C(14)- -C(21) 3.147(10) Å). In the dominant (67.0(7)%) conformer, this approximate molecular symmetry is destroyed and the latter torsion angle is "relaxed" to C(7)−Se(8)−C(9)−C(34) −49.1(4)° (cf. C(7)- -C(34) 3.236(12) Å). Also, two close Se- -C intramolecular distances in the minor conformer (Se(1)- -C(15) 3.489(16) Å and Se(18)- -C(15) 3.476(11) Å) increase to 4.221(5) and 4.258(8) Å, respectively, for Se(1)- -C(5) and Se(8)- -C(5) in the major conformer. In addition, two intramolecular C- -C contacts occur in the major conformer (C(3)- -C(6) 3.331(10) Å and C(6)- -C(9) 3.313(9) Å) which are not significant in the minor conformer (C(3)- -C(16) 3.427(14) Å and C(9)- -C(16) 3.464(16) Å). The molecules 2,3,9,10-dibenzo-6,13-dihydroxy-1,4,8,11-tetrathiacyclotetradecane and 2,3,9,10-dibenzo-6,13-dihydroxy-1,4,8,11-tetrathiacyclotetradecane 4-oxide,[84] both display conformations similar to that of the minor conformer in **1**. It seems reasonable that the shorter S−C bonds (compared to the Se−C bonds in

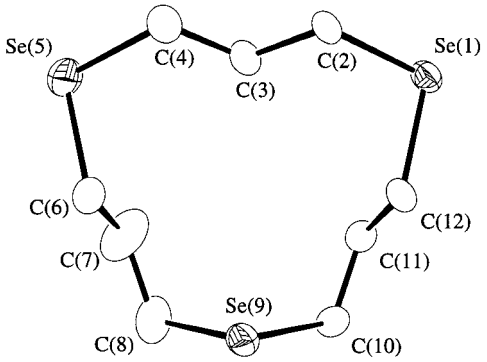

Figure 3. Molecular structure of **2**. 50%-enclosure thermal ellipsoids of the non-hydrogen atoms are shown.

1) would increase the severity of nonbonded contacts, such as those to C(6) in the major conformer of **1**, thus disfavoring the corresponding conformer in the analogous sulfur compounds. The only intermolecular distance in the solid-state structure of **1** (either Se- -C or C- -C) significantly less than the appropriate sum of van der Waals radii is C(15)- -C(12)′ (3.305(15) Å; where ′ indicates $x + {}^1/_2, -y, z$). The sums of accepted van der Waals radii are 3.40 Å for C- -C and 3.60 Å for Se- -C.[85]

An interesting feature of **1** is that the two arene rings are nearly coaxial. The dihedral angle between the planes of the arene rings is 6.0(3)°. An intriguing speculation is the possibility of forming chelating bis(arene)metal complexes with this molecule. The arene rings' centroids are separated (intramolecularly) by 5.05 Å, and the shortest inter-ring C- -C distances range from 4.902(9) Å (C(21)- -C(31)) to 5.253(9) Å (C(24)- -C(34)). The rings are thus a little too far apart to form stable chelating bis(arene)metal sandwich complexes without some conformational change in the $Se(CH_2)_3Se$ chains, but the molecule may be flexible enough to accommodate this. By comparison, in 2,3,9,10-dibenzo-6,13-dihydroxy-1,4,8,11-tetrathiacyclotetradecane,[84] the distance between the arene rings is reported to be in the range 4.3−4.4 Å.

The molecular structure of **2** is shown in Figure 3. Selected bond distances, bond angles, and torsion angles are given in the Supporting Information. The molecule has no crystallographic symmetry but does have approximate local mirror (*Cs* or *m*) symmetry across a plane passing through Se(9) and C(3). The analogous 12S3 compound has been found to display 2-fold rotational symmetry (*C*2 or 2).[86] In **2**, every C−Se−C−C segment has the preferred gauche torsional arrangement,[7] whereas the molecule of 12S3 with *C*2 symmetry has two anti C−S−C−C segments. The only intermolecular distances significantly less than the sums of accepted van der Waals radii are Se(1)- -Se(1)′ 3.774(1) Å (′ indicates $-x, y - {}^1/_2, -z$), Se(1)- -Se(1)″ 3.774(1) Å (″ indicates $-x, y + {}^1/_2, -z$), and Se(1)- -Se(5)† 3.731(1) Å († indicates $-x + {}^1/_2, y + {}^1/_2, z - {}^1/_2$). Twice the accepted van der Waals radius of selenium is 3.8 Å.

The crystal structure of **3** was found to be similar to, but not isomorphous with, that of 1,5,9,13-tetraselenacylcohexadecane (16Se4).[9] The asymmetric unit contains 1.5 molecules. Thus, there are two crystallographically distinct molecules in a ratio of 2:1. One molecule has no crystallographic symmetry, while the other molecule is centered on the crystallographic 2-fold axis. There was not the extensive orientational and/or confor-

(84) Comba, P.; Fath, A.; Kuhner, A.; Nuber, B. *J. Chem. Soc., Dalton Trans.* **1997**, 1889.
(85) Bondi, A. *J. Phys. Chem.* **1964**, *68*, 441.
(86) Rawle, S. C.; Admans, G. A.; Cooper, S. R. *J. Chem. Soc., Dalton Trans.* **1988**, 93.

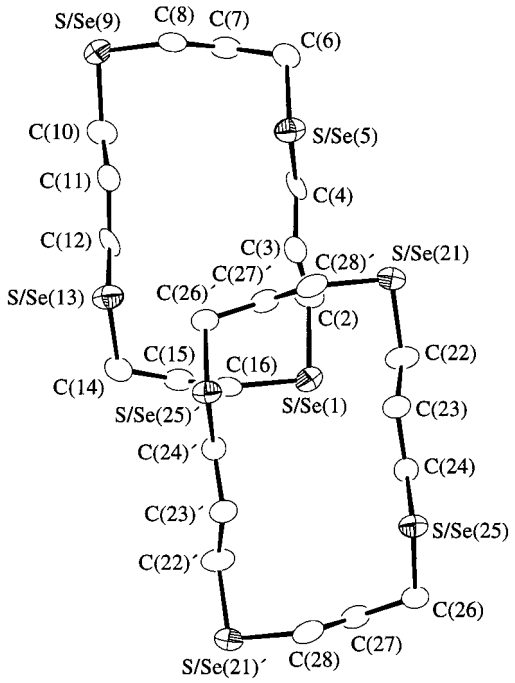

Figure 4. The two crystallographically distinct molecules of **3** viewed along the *b* axis. 50%-enclosure ellipsoids for the non-hydrogen atoms are shown.

mational disorder of the type exhibited by 16Se4;[9] however, there was disorder corresponding to the interchange of selenium and sulfur at the chalcogen atom sites. While the difference in covalent radii for sulfur and selenium would, in fact, not permit precise superposition of the atomic sites, it is not sufficiently large to allow any individual sites to be resolved, particularly since this type of disorder may correspond to the superposition of two different orientations of each of two different conformations of the molecule (i.e., multiple sites for each atom, probably separated by less than 0.14 Å). For the crystallographically asymmetric ring, the refined occupancy ratios S/Se (0.243/0.757(4) for S/Se(1) and 0.417/0.583(4) for S/Se(5); conversely, 0.757/0.243 for S/Se(9) and 0.583/0.417 for S/Se(13)) for the chalcogen sites suggest that at least three (and probably all) of the four possible arrangements are contributing to the average structure. The crystallographic 2-fold symmetry of the other independent molecule requires that its S/Se ratios be 0.5/0.5.

The two independent molecules of **3** are shown in Figure 4. Both are [3535] quadrangles, as was also found for 16Se4.[7] While the disordered structural models for these molecules display approximate (S/Se(1)−C(16)) and precise (S/Se(21)−C(28)) molecular 2-fold rotational point symmetry, the substitution pattern (1,5-Se-9,13-S) in any individual molecule having this conformation requires it to be asymmetric. Selected intramolecular distances and angles of **3** are given in the Supporting Information. The weighted-mean chalcogen atom site to carbon atom site "bond distances" are reasonable (range: S/Se(9)−C(10) 1.847(13) Å to S/Se(1)−C(2) 1.938(13) Å) and display the expected correlation with the fractional selenium occupancy parameters. Typical distances for Se−C are about 1.96 Å and for S−C are about 1.82 Å. The C−C bond distances in **3** range from 1.47(2) Å to 1.55(2) Å. The C−S/Se−C bond angles range from 97.7(6) to 101.2(6)°; the C−C−S/Se angles, from 107.2(8) to 116.7(9)°; and the C−C−C angles, from 109.8(11) to 113.7(11)°. There are only three intermolecular distances which appear significantly shorter than the appropriate sums of accepted van der Waals radii: S/Se(1)- -S/Se(1)′ 3.536(3) Å (′ = 2 − *x*, *y*, 1.5 − *z*); S/Se(5)- -S/Se(13)″ 3.505(3) Å (″ = −0.5 + *x*, 0.5 − *y*, −0.5 + *z*); S/Se(25)- -S/Se(25)† 3.558(4) Å († = 2 − *x*, −*y*, 2 − *z*). The accepted van der Waals radius of selenium is 1.90Å, and that of sulfur is 1.80 Å. Similar Se- -Se contacts were observed for 16Se4.[9]

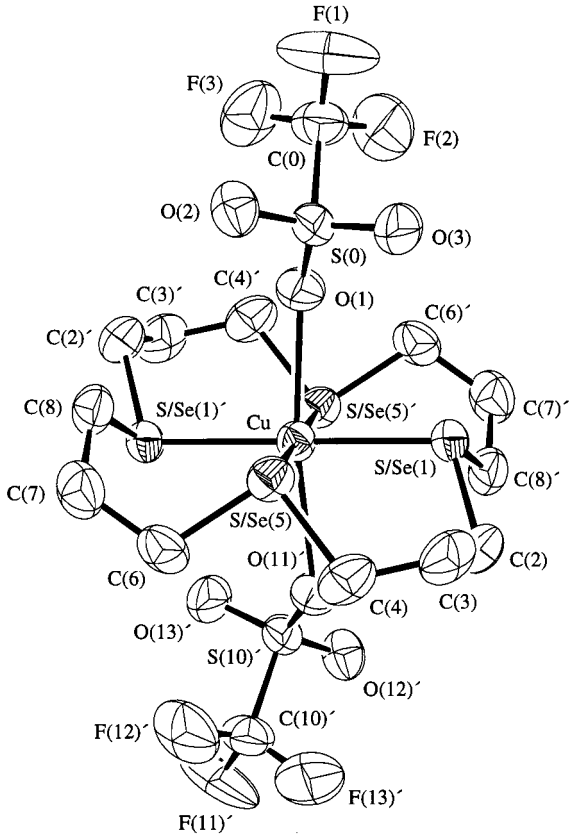

Figure 5. Molecular structure of **4**. 50%-enclosure ellipsoids are shown for the non-hydrogen atoms. For clarity of presentation, the two disordered orientations of the SO_3CF_3 group are depicted exclusively on opposite sides of the molecule.

Like the structure of **3**, that of **4** has 0.5/0.5 S/Se occupancy disorder, which is spatially unresolved. The average molecular structure has inversion symmetry. The molecular structure of **4** is depicted in Figure 5. For clarity of presentation, the alternate orientations of the disordered SO_3CF_3 group are shown exclusively on opposing sides of the copper atom, which is, in practice, situated on a crystallographic inversion center. This structure differs from that of [Cu(16Se4)][$(SO_3CF_3]_2$[12] in the orientations of the SO_3CF_3 groups relative to the rest of the molecule. The configuration of the bonding of the coronand to copper, denoted as c,t,c (cis,trans,cis) to describe the relative orientations of the adjacent pyramidal chalcogen centers, and its [4444] conformation are the same as those in both [Cu(16Se4)][$SO_3CF_3]_2$ and [Cu(16S4)][$ClO_4]_2$.[87] Selected intramolecular distances and angles for **4** are listed in the Supporting Information. All the molecular dimensions of **4** agree reasonably with expected values. The weighted-mean Cu−S/Se distances are S/Se(1)−Cu 2.4095(7) Å and S/Se(5)−Cu 2.4136(6) Å. These are intermediate between the Cu−Se bond lengths in [Cu(16Se4)][$SO_3CF_3]_2$ (2.4593(6) and 2.4554(6) Å) and the Cu−S bond lengths in [Cu(16S4)][$ClO_4]_2$ (2.3314(13) and 2.3874(17) Å). The mean Cu−O bond length in **4** (2.46 Å) is indistinguishable from that in [Cu(16Se4)][$SO_3CF_3]_2$ (2.464(5) Å). The weighted-mean chalcogen atom site to carbon atom site "bond

(87) Pett, V. B.; Diaddario, L. L., Jr.; Dockal, E. R.; Corfield, P. W.; Ceccarelli, C.; Glick, M. D.; Ochrymowycz, L. A.; Rorabacher, D. B. *Inorg. Chem.* **1983**, *22*, 3661.

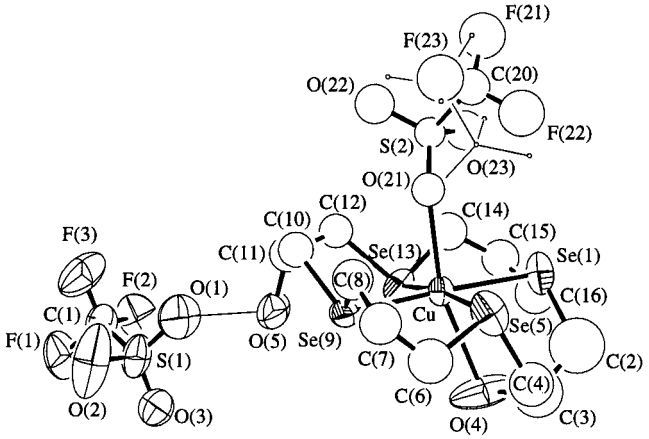

Figure 6. Molecular structure of **5**. 50%-enclosure ellipsoids or spheres shown represent a degree of unmodeled disorder. For clarity of presentation, one (44.9(6)% occupancy) of the two disordered orientations of the coordinated SO_3CF_3 group (partially obscured) is depicted by small spheres and line bonds. The oxygen atoms involved in the interionic hydrogen bond are connected with a line.

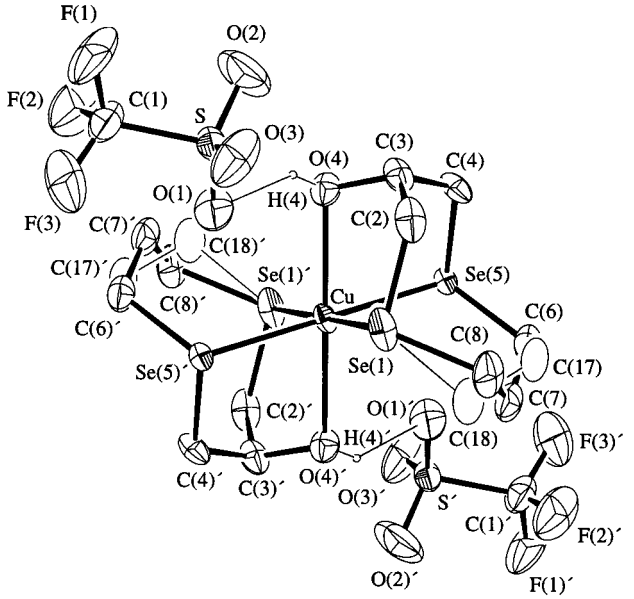

Figure 7. Molecular structure of **6**. Boundary ellipses and single line bonds only are shown for the 12.9(6)% conformation of the disordered 1,3-propanediyl segment. 50%-enclosure ellipsoids for the non-hydrogen atoms and a sphere of arbitrary radius for the hydroxyl hydrogen atom are depicted. Lines denote the O(4)−H(4) bond and the hydrogen bond to O(1).

distances" range from S/Se(1)−C(2) 1.897(4) Å to S/Se(1)−C(8) 1.911(4) Å. The C−C bond distances in **4** range from 1.506(6) to 1.523(6) Å. The C−S/Se−C bond angles are 95.6-(2) and 94.6(2)°, the C−C−S/Se angles range from 110.6(3) to 113.7(3)°, and the C−C−C angles are 114.4(4) and 114.5-(3)°. There are no significant intermolecular contacts.

The molecular structure of **5** is shown in Figure 6. Significant discussion of the molecular dimensions is precluded by extensive, incompletely modeled disorder exhibited by the structure. Nonetheless, the connectivity and stereochemistry are clearly revealed. Detailed results of this structure determination are available in the Supporting Information. The configuration of the complex with regard to the stereochemistry at the selenium atoms (c,t,c) is analogous to that in **4**. The hydroxyl substituents of the coronand ligand have a mutual cis relationship. This combination of stereochemical features allows only one hydroxyl group to chelate to the copper center, imposing a boat conformation on the corresponding Se−Cu−Se−C−C−C ring. The coordination environment of the copper ion can also be described as approximately tetragonally distorted octahedral, with a hydroxyl oxygen atom and an SO_3CF_3 oxygen atom each occupying one of the pseudoaxial positions. The noncoordinated hydroxyl group forms a hydrogen bond to an oxygen atom of the noncoordinated $SO_3CF_3^-$ ion. The chelating hydroxyl group is displaced somewhat from the ideal axial position as a consequence of constraints required for coordination of the selenium atoms. By comparison, in the analogous complex of copper(II) perchlorate with *cis*-16S4(OH)$_2$ (where *cis*-16S4-(OH)$_2$ = *cis*-3,11-dihydroxy-1,5,9,13-tetrathiacyclohexadecane), neither of the hydroxyl groups coordinates to Cu but rather the perchlorate ions coordinate in both axial positions as in the nonhydroxylated compounds.[88]

The complex cation of **6** and its associated hydrogen-bonded anions are shown in Figure 7. There is conformational disorder resolved for an ethyl group. Selected bond distances, bond angles, and torsion angles are given in the Supporting Information. The structure of the complex cation of **6** is very similar to that of [Cu(8S2(OH))$_2$][ClO$_4$]$_2$[89] (where 8S2(OH) = 3-hydroxy-1,5-dithiacyclooctane). Both are centrosymmetric and have an approximately tetragonally distorted octahedral coordination of the copper ion, with the hydroxyl oxygen atoms occupying the more weakly bound axial positions. The Cu−O bond distance in **6** (2.358(3) Å) is not significantly different from that in [Cu-(8S2(OH))$_2$][ClO$_4$]$_2$[89] (2.350(2) Å). In **6**, the Cu−O(4) bond is tilted 13.3° from the normal to the $CuSe_4$ plane, while the analogous angle in [Cu(8S2(OH))$_2$][ClO$_4$]$_2$[89] is 13.6°. In both structures, the hydroxyl groups form hydrogen bonds of comparable strengths to neighboring anions. A notable difference is that, whereas **6** displays predominantly (87.1(6)%) the chair−chair conformation with a lesser (12.9(6)%) contribution from a boat−chair form for the eight-membered ring, [Cu-(8S2(OH))$_2$][ClO$_4$]$_2$[89] displays only the boat−chair conformation, as does its 3-methoxy analogue.[83] There are no atypical bond distances or bond angles in the structure of **6**. Other than the H-bonded interactions, the only interionic distances significantly less than the appropriate sums of van der Waals radii are Se(5)- -Se(5)′ 3.499(1) Å (′ indicates $-x$, $1-y$, $-z$) and Se(5)- -O(1)″ 3.084(3) Å (″ indicates $1-x$, $2-y$, $-z$).

The crystal structure of **7** displays S/Se site occupancy disorder, some resolved conformational disorder of a propyl subchain, and orientational disorder of the $SO_3CF_3^-$ anion. Despite this, significant configurational and conformational details can be interpreted. The structure of **7** contains discrete complex cations and anions. There are only two interionic separations (for which at least one site is not a component of disorder) which are significantly, albeit slightly, less than the appropriate sums of van der Waals radii (Se(9)- -C(140)′ 3.50-(3) Å and O(11)- -C(12)″ 3.097(12) Å). As in the case of **8** (see below), the coordination of Cu(I) by the coronand is tetrahedral and the complex stereochemistry is denoted t,t,t. Selected intramolecular distances and angles are given in the Supporting Information**.** Bond lengths and angles do not deviate significantly from expected values. The structure of the predominant (71.9(9) %) conformation of the complex cation of **7** is depicted in Figure 8. Ignoring the variable S/Se site

(88) Munakata, M.; Wu, L. P.; Yamamoto, M.; Kuroda-Sowa, T.; Maekawa, M. *J. Chem. Soc., Dalton Trans.* **1995**, 3215.

(89) Musker, W. K.; Olmstead, M. M.; Kessler, R. M. *Inorg. Chem.* **1984**, *23*, 1764.

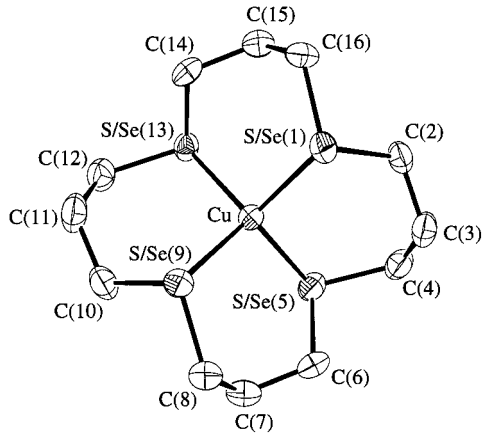

Figure 8. Predominant cationic structure of **7**. 50%-enclosure ellipsoids are shown for non-hydrogen atoms.

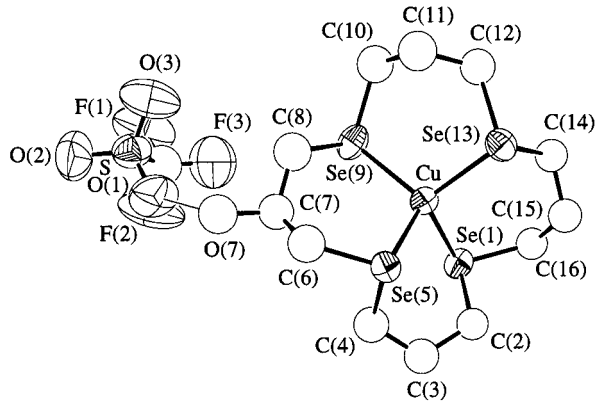

Figure 9. Predominant ion-pair combination of **8**. 50%-enclosure ellipsoids or spheres for non-hydrogen atoms are shown. A single line represents the hydrogen bond from O(7) to O(1).

substitution, this conformation displays approximate 2-fold rotational symmetry about an axis which intersects the midpoint of the S/Se(1) to S/Se(9) vector and Cu (i.e., normal to the projection shown). The alternate conformation (28.7(9) %) replaces C(14)−C(15)−C(16) with C(140)−C(150)−C(160) and is asymmetric. Neither of these two conformations matches those found for **8** (see below).

The crystal structure of **8** displays conformational disorder, resolved for one C_3 subchain, as well as positional disorder of the hydroxyl substitutent. The structure of **8** contains hydrogen-bonded ion pairs. The predominant combination is shown in Figure 9. The coordination at Cu is tetrahedral. The configuration in which the coronand complexes Cu is denoted as t,t,t. Selected intramolecular distances and angles are given in the Supporting Information. The site of hydroxyl substitution in the crystal structure of **8** varies among O(7) (56.6(13)%; shown in Figure 9), the alternate position on the same carbon atom (22.3(12)%), denoted O(107), and two reasonably situated lesser contributors—O(15) (11.9(12)%) and O(11) (9.3(11)%), bonded to C(15) and C(11), respectively. O(7), O(11), and O(15) are all in pseudoequatorial positions (directed away from Cu when viewed as in Figure 9) and are located such that each would form a hydrogen bond with an oxygen atom from an adjacent anion (O(7)- -O(1) 2.611(15) Å, O(11)- -O(1)′ 2.73(5) Å (′ indicates $1 - x, -y, 1 - z$); O(15)- -O(3)″ 2.84(6) Å (″ indicates $x, y, -1 + z$)). In contrast, O(107) is in the pseudoaxial position on C(7) and displays a weaker hydrogen-bonded interaction (O(107)- -F(2)† 2.92(3) Å († indicates $1 - x, 1 - y, 1 - z$)). This pseudoaxial positioning of O(107) also places it 3.16(4) Å from Se(9) and 3.35(3) Å from Se(5) (both intramolecular distances). Only the former distance is significantly less than the sum of the oxygen and selenium van der Waals radii (3.42 Å). The nonbonding pair of electrons of Se-(9) is on the same side of the ring as is O(107), whereas that of Se(5) is not, suggesting that the short distance to Se(9) may represent a weakly attractive interaction involving the hydroxyl hydrogen atom. The nearest anionic oxygen atom to O(107) is O(1) (3.15(4) Å). Clearly, the derived errors in these distances are underestimated, particularly since the disorder would likely result in slightly differing orientations and positions for the $SO_3CF_3^-$ ion. This ion was reasonably modeled with single atom sites whose anisotropic displacement parameters may account for multiple sites. There are no other interionic distances significantly less than the appropriate sums of atomic van der Waals radii. Further disorder replaces the segment C(10)−C(11)−C(12) (65.4(14)%) by a C_3 arrangement, denoted C(110)−C(111)−C(112). It may be no coincidence that the occupancy for C(10)−C(11)−C(12) refined to a value equal to the sum of the refined occupancies of O(7) and O(11). One possible interpretation of this is that the structure occurs in the C(110)−C(111)−C(112) form exclusively when the hydroxyl group is located at either O(107) or O(15). The two different C_3 arrangements represent alternate "half-boat" conformations of the associated $SeCuSeC_3$ six-membered ring. If anions and the ring substituents are ignored, the skeletal Cu(16Se4) complex still displays only 1 (*C*1) point symmetry for either conformation; however, the two conformations are approximately related by a 180° rotation of the complex about the axis passing through Cu and C(3). Thus, the forms with oxygen at O(7) or O(15) could merely represent different orientations of the cation, while the O(7)- and O(107)-substituted forms differ in conformation (and orientation). On the other hand, substitution at O(11) produces a form enantiomeric with, and also differing in conformation (and orientation) from, the others.

As might be expected, the sequences of bond torsion angles about the coronand rings in the conformations found for **7** and **8** display similar features (see Supporting Information). These conformations generally display a repeating pattern of three gauche torsional arrangements followed by one anti, where the first and third always have opposite signs (e.g., $G^+G^-G^-A$ etc.). The chalcogen atoms prefer positions between gauche and anti torsional arrangements (denoted GA). This is strictly obeyed in the predominant conformation of **7** (Figure 8), but in its other conformation, and in the two observed for **8**, there is an additional anti relationship such that one chalcogen atom in each case resides in a position denoted AA. In these cases, the bond torsion angles show larger deviations from 180°.

For free coronand ligands, it has been found that the chalcogen atoms prefer GG sites.[9,90] In coronand complexes with relatively small ring sizes, such an arrangement does not occur, since it would require the chalcogen atom to have its nonbonded electron pairs exo with respect to the centrally located metal cation. Thus, for square planar coordination of 16S4[87] or 16Se4,[12] the chalcogen atoms are located in AA sites. Tetrahedral coordination, as described herein, apparently favors positioning of S or Se in GA sites. It would be of interest to compare these conformations and configurations with those for the potentially symmetrical species $[Cu(16Se4)]^+$ or $[Cu(16S4)]^+$; however, suitable crystals containing these complex cations have not been obtained. An earlier attempt to prepare $[Cu(16Se4)]^+$ resulted in a compound that had the correct stoichiometry but

(90) Wolf, R. E., Jr.; Hartman, J. R.; Storey, J. M. E.; Foxman, B. M.; Cooper, S. R. *J. Am. Chem. Soc.* **1987**, *109*, 4328.

which contained a three-dimensionally polymeric cation in which each copper atom was tetrahedrally coordinated to selenium atoms from four different 16Se4 rings,[14] which remained in the free-ligand conformation. 16S4 has also been found to form a polymeric complex cation with Cu(I).[91]

Conclusions

The synthesis, characterization, redox properties, and X-ray crystal structures of the new selenium coronands **1**, **2**,[10] and **3** and the copper(II) and copper(I) complexes **4**, **5**, **6**, **7**, and **8** have been described. X-ray crystallographic studies have shown that complexes **4**, **5**, and **6** have typical tetragonally distorted octahedral coordination environments of Cu(II) and that **7** and **8** are both tetrahedral Cu(I) coronand complexes with typical t,t,t configurations. Compounds **2**, **3**, **9**,[11] and **10**[11] and the dicationic compound **11** have been examined by solid-state ^{13}C and ^{77}Se NMR spectroscopy. For the neutral compounds **2**, **3**, **9**,[11] and **10**,[11] ^{77}Se shifts are in the range characteristic of dialkyl selenides.[57] The dicationic compounds **11** and 16Se4$(SO_3CF_3)_2$[16] resonate at lower field, reflective of a contribution from the transannular Se−Se bonds present in these ions.[16,58,59]

Cyclic voltammetry of the Cu(II) complexes of selenium coronands has shown that the redox reaction of the $Cu^{II}L/Cu^{I}L$ pair is chemically reversible. This reversibility may result from the stabilization of Cu(I) ions through coordination to the selenium coronands. The preferential stabilization of Cu(I) ions by the selenium coronands is also indicated by the spontaneous reduction of the Cu(II) selenium coronand complexes to Cu(I) selenium coronand complexes.[16] The configurational changes between copper(II) complexes (octahedral or tetragonal configurations)[78] and copper(I) complexes (tetrahedral configurations) are reflected in the cyclic voltammograms of the Cu(II) selenium coronand complexes. The quasi-reversible cyclic voltammograms observed for the copper(II) complexes of selenium coronands indicate that the configurational changes are slower than the electron transfers to the electrodes. Our copper complexes are analogous to Rorabacher's copper(II/I) complexes of macrocyclic tetrathiaether ligands, in that different conformational isomers of the complexes are present. The electron-transfer reactions follow a dual-pathway square-scheme mechanism, whereby they are faster than the conformational interconversions between isomers under certain conditions.[80,81]

Acknowledgment. We are grateful to the Natural Sciences and Engineering Research Council of Canada for financial support.

Supporting Information Available: Text and tables giving additional crystallographic details and tables listing atomic coordinates, anisotropic displacement parameters, distances, angles, and least-squares planes. This material is available free of charge via the Internet at http://pubs.acs.org.

IC991345P

(91) Musker, N. K.; Gorewit, B. V. *J. Coord. Chem.* **1976**, *5*, 67.